Computer Modeling in Engineering & Sciences

Tech Science Press

DOI: 10.32604/cmes.2024.047156

ARTICLE

Prospect Theory Based Individual Irrationality Modelling and Behavior Inducement in Pandemic Control

Wenxiang Dong and H. Vicky Zhao*

Department of Automation, BNRist, Tsinghua University, Beijing, 100084, China

*Corresponding Author: H. Vicky Zhao. Email: vzhao@tsinghua.edu.cn

Received: 27 October 2023 Accepted: 04 January 2024 Published: 16 April 2024

ABSTRACT

Understanding and modeling individuals' behaviors during epidemics is crucial for effective epidemic control. However, existing research ignores the impact of users' irrationality on decision-making in the epidemic. Meanwhile, existing disease control methods often assume users' full compliance with measures like mandatory isolation, which does not align with the actual situation. To address these issues, this paper proposes a prospect theory-based framework to model users' decision-making process in epidemics and analyzes how irrationality affects individuals' behaviors and epidemic dynamics. According to the analysis results, irrationality tends to prompt conservative behaviors when the infection risk is low but encourages risk-seeking behaviors when the risk is high. Then, this paper proposes a behavior inducement algorithm to guide individuals' behaviors and control the spread of disease. Simulations and real user tests validate our analysis, and simulation results show that the proposed behavior inducement algorithm can effectively guide individuals' behavior.

KEYWORDS

Disease spread; behavior model; irrationality; prospect theory

1 Introduction

The outbreak of COVID-19 has led to a severe public health crisis and great economic losses. Governments worldwide have taken various measures, including lockdowns and mandatory quarantines, to inhibit the spread of the disease. However, individuals may not comply with these policies, as many have their own opinions and preferences. In such public health crises, individuals tend to act irrationally, such as excessive panic in an epidemic outbreak and underestimation of the dangers of the epidemics in its later spread, which can significantly affect individuals' decisions and ultimately affect the spread of the epidemic. Moreover, individuals' behaviors and the epidemic affect each other. For example, individuals' behaviors such as social distancing, wearing masks, and isolating can inhibit the spread of the epidemic, and individuals tend to choose protective behaviors when the pandemic is more severe. Therefore, it is crucial to model individuals' behaviors during the epidemic and determine how to control the spread of the epidemic by guiding individuals' behaviors without resorting to mandatory measures.

1.1 Literature Review

In the following, this paper reviews recent works on epidemic control over networks, individual behavior modeling during an epidemic, and irrational behavior modeling.

1.1.1 Epidemic Control

There are numerous studies on how to control the epidemic spread over networks, and many attempted to inhibit the epidemic spread on a network by removing nodes. Wang et al. pointed out that the epidemic spread on a network is highly correlated with the largest eigenvalue of the graph's adjacency matrix [1]. Based on this, existing studies [2–5] attempted to manipulate the adjacency matrix's eigenvalues by removing nodes to minimize the likelihood of epidemic outbreaks. Meanwhile, some studies [6–8] investigated macro-level approaches to control epidemic spread, such as restricting population movement or implementing proportional quarantine. Besides, studies [9–12] examined the impact of isolation and immunization on disease spread.

The studies on epidemic control investigated how to control the spread by isolating individuals, restricting population movement, etc. However, these studies all assumed that individuals would comply with the control policies, which is usually not the actual situation. In reality, individuals have their own ideas and may not necessarily obey policies such as isolation and movement restrictions.

1.1.2 Individual Behavior Modeling during an Epidemic

Some prior works attempted to model individual behaviors during an epidemic. The studies [13–17] showed that as the proportion of infected individuals in the environment increases, people are more likely to adopt protective behaviors. Zhang et al. assumed that individuals would be more likely to take protective behavior when there is a large proportion of infected neighbors [14], and they analyzed the effect of individual protective behavior on epidemic spread. The model proposed in [15] assumed that an individual's adoption of protective behavior is affected by the proportion of infected neighbors, as well as regional and global infection rates. The studies [18–20] observed that information dissemination also affects individual protective behavior during the epidemic.

These studies modeled and analyzed individuals' behavioral choices in the epidemic. However, they did not consider the common and critical issue of individual irrationality, which can significantly affect their decision-making process during an epidemic.

1.1.3 Irrational Behavior Modeling

Individuals usually resort to irrational decision-making when confronted with risks, such as the potential for infection during an epidemic. For instance, many people may be overly panicky in the early stages of an epidemic and may underestimate the risk of the epidemic in the later stages. A challenge here is how to mathematically model such irrational behaviors. Prospect theory provides theoretical models to quantify how individuals tend to overestimate small probabilities and underestimate high probabilities [21–25]. It is crucial to analyze the impact of this irrationality on individuals' decisions. The study [26] considered risk aversion during the consensus reaching process (CRP) in group decision-making. The studies [27–29] analyzed the impact of irrationality on individuals' decisions on whether to take vaccination during an epidemic, and they assumed that this is a one-time binary decision problem where users only make one binary decision during the entire epidemic. However, in reality, individuals can take multiple protective behaviors, such as wearing a mask, washing hands, and isolating at home, and they need to continuously decide whether to take such protective behaviors and which behavior to take during the entire epidemic. Individuals may choose to adopt the highest-level protective measures such as self-isolation when the epidemic is rapidly spreading, and choose to not take any protective behaviors when the epidemic is declining.

The existing studies modeled individuals' irrationality and simple decisions such as whether to take a vaccination. However, they did not consider the continuous interaction and mutual influence between the epidemic spread and individual choices over time in the context of irrational behaviors.

1.2 Our Contribution

Our work differs from prior works in two aspects. First, prior works on individual behavior modeling in epidemics either ignore the impact of irrational decision-making or fail to consider the continuous interaction and mutual influence between the epidemic spread and individual behaviors. In this paper, the prospect theory is applied to model individuals' irrational decisions during an epidemic and the co-evolution of individuals' behaviors and the epidemic. We theoretically analyze the impact of the individuals' irrationality on their decisions as well as the epidemic. Second, existing works on epidemic control assume individuals' absolute compliance with the government's policies such as mandatory isolation. In this paper, based on the individual behavioral model, we propose an effective method to guide individuals' behaviors and control the epidemic spread. In contrast to prior approaches, our disease spread control method does not rely on mandatory measures.

The main contributions of our work are:

- We build an M-choice epidemic-behavior co-evolution model to simulate individuals' irrational decision-making and analyze their impact on the epidemic. We theoretically analyze the co-evolution of user behavior and epidemic and its steady state. Also, the impact of irrationality on individuals' behaviors and disease spread is theoretically analyzed.
- Given the above individual behavior model, we propose a behavior inducement algorithm to guide individuals' decisions to control the epidemic.
- We validate our individual behavior model and behavior inducement algorithm through simulations. In addition, we use real user tests to validate the conclusions about the impact of irrationality on individuals' behavior.

The rest of the paper is organized as follows. Section 2 introduces our proposed epidemic-behavior co-evolution model. Section 3 analyzes the steady state of the epidemic-behavior dynamics and the influence of irrationality. Section 4 presents the behavior inducement method to control the disease spread. Section 5 provides the simulation results. Section 6 shows the results of real user tests, and conclusions are given in Section 8. The important notations of this paper are listed in Table 1.

Table 1: Notations

Notations	Meaning
$s(t)$, $i(t)$	The fractions of susceptible and infected individuals at t
$a_1, a_2, \ldots, a_M$	The possible behaviors individuals can adopt
$x_j(t)$	The proportion of susceptible individuals adopting action a_j at time t
c_j	The actual payoff when behavior a_j is adopted
c_n	The loss of being infected
β_j	The infection rate when the individual takes action a_j

(Continued)

Table 1 (continued)

Notations	Meaning
γ	The recovery rate
N	The number of individuals
$\bar{k}$,$\bar{d}$	The degree of the physical contact network and the information network
$u^E(x)$, $u^P(x)$	The value function of the expected utility theory and prospect theory
$\omega(p,\alpha)$	The weighting function of the prospect theory
α	The irrationality coefficient
(i^E, x_1^E)	The steady state of the 2-behavior model following the expected utility theory
(i^P, x_1^P)	The steady state of the 2-behavior model following the prospect theory

2 The M-Choice Epidemic-Behavior Co-Evolution Model

During an epidemic, individual behavioral choices and the spread of the disease mutually influence each other. When the probability of infection and the potential losses are high, people tend to adopt protective behaviors, which in turn can inhibit the epidemic spread. In this section, we propose a model to capture the co-evolution of individual behavioral choices and disease spread during a pandemic. We consider irrational behavior in our model and use the model with rational behavior assumption as a baseline to analyze the impact of irrationality on the evolutionary dynamics of the epidemic and its steady states. Based on the model presented in [30], we assume that individuals have a choice among M possible behaviors based on the severity of the epidemic, and these behavioral choices, in turn, affect the epidemic spread.

Following the work in [19], two undirected networks are used in this paper to represent the connections among individuals. The first network is the physical contact network where the disease spreads. The second network is the information network where individuals exchange information about their current health state and behavioral choices. It is worth noting that the two networks are different. In reality, an individual may get infected by strangers in a restaurant or on a bus, while their behaviors will not be influenced by these strangers since they have not interacted with them. Similarly, individuals' decisions may be influenced by their friends on the Internet without any physical contact with each other. To simplify the analysis, we make the assumption that both the physical contact network and the information network are regular networks consisting of N nodes, where each node represents an individual. In a regular network, each node has a fixed degree, denoted as $\bar{k}$ for the physical contact network and $\bar{d}$ for the information network. As individuals communicate with each other in the information network, we assume that they have knowledge of the health states of their neighbors in the information network. However, in the physical contact network, there is information exchange, and we assume that individuals do not have knowledge of the health states of their neighbors. In the following, we will use the terms "graph" and "network" interchangeably, and the terms "node", "user", and "individual" interchangeably.

Our model consists of two interconnected parts: the disease spread model and the behavior change model. The disease spread model quantifies how the epidemic spreads through the network given the current behaviors of all individuals, and the behavior change model describes how individuals update their behaviors based on the current number of infected individuals and the behaviors of their neighbors. The illustration of our model is in Fig. 1. In the following, the two components of our model will be introduced in detail.

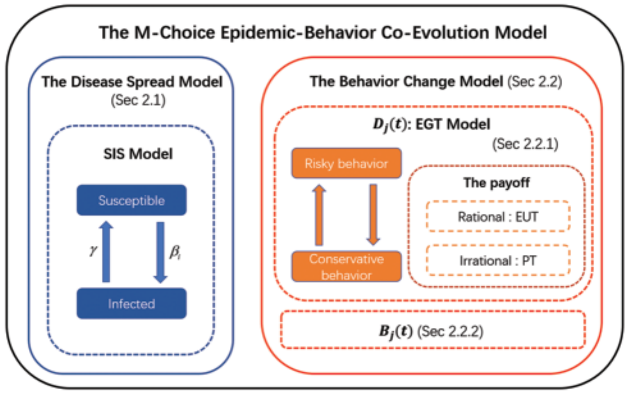

Figure 1: The proposed M-choice epidemic-behavior co-evolution model

2.1 The Disease Spread Model

We use the classic Susceptible-Infected-Susceptible (SIS) model to depict disease spread, which describes the disease spread process using differential equations. In addition to depicting disease spread, this method of differential equations has a wide range of applications, such as describing the spread of viruses in the body [31,32] and the evolution of opinions [33,34]. In the SIS model, each individual can be in one of two health states: susceptible or infected. We divide time into slots of equal length. At each time slot, a susceptible individual can be infected by an infected individual at a certain infection rate, and an infected individual recovers at a certain recovery rate. We assume that susceptible individuals can adopt different protective measures to reduce their risk of infection, and they have a total of M possible behavioral options $\{a_1, a_2, ..., a_M\}$. For example, some may take the epidemic very seriously and adopt self-quarantine to avoid contact with infected individuals; some may adopt medium-level protective behaviors such as wearing masks when going out and washing hands frequently; while others may take no protective behaviors and act as if the epidemic does not exist. To simplify the analysis, we also assume that all susceptible individuals taking action a_j have the same infection rate β_j. For those already infected with the disease, we consider the worst-case scenario where they do not take any protective behavior such as home isolation to prevent the disease from further spreading. This assumption is grounded in the understanding that infected individuals might not possess the same level of motivation or necessity to embrace protective measures since they are already infected. We also assume that all infected people have the same recovery rate γ to simplify the analysis. Let $s(t)$ and $i(t)$ be the fractions of susceptible and infected individuals respectively at time t, while $x_j(t)$ denotes the fraction of individuals adopting action a_j among all susceptible individuals at time t. Then the mean-field equation of the disease spread is:

$$\frac{ds}{dt} = \gamma i(t) - s(t)i(t)\bar{\beta}\bar{k}, \quad \text{and} \quad \frac{di}{dt} = s(t)i(t)\bar{\beta}\bar{k} - \gamma i(t), \tag{1}$$

where $s(t) + i(t) = 1$ and $\bar{\beta} = \sum_{j=1}^{n} \beta_j x_j(t)$. By substituting $s(t) = 1 - i(t)$ into (1), the differential equation modeling the disease spread can be obtained:

$$\frac{di(t)}{dt} = i(t)(1 - i(t))\bar{\beta}\bar{k} - \gamma i(t). \tag{2}$$

2.2 The Behavior Change Model

The individual behavior model quantifies the dynamics of $\{x_j(t)\}, j = 1...M$, which represents the proportion of susceptible individuals adopting action a_j at time t. The change in $x_j(t)$ can be attributed to two main factors. First, individuals may change their decisions over time in response to the severity of the epidemic and the influence of their neighbors' behaviors. We use $D_j(t)$ to represent this part of the change in $x_j(t)$. Meanwhile, due to nodes' changes in their health state, the proportion of susceptible individuals adopting different behaviors may also change. For example, a susceptible individual who was taking action a_j at time $t-1$ may become infected at time t, or an infected person recovers at time t and decides to take action a_j. We use $B_j(t)$ to represent this part of the change in $x_j(t)$. Then we have:

$$\frac{dx_j(t)}{dt} = D_j(t) + B_j(t). \tag{3}$$

In Section 2.2.1, we focus on modeling $D_j(t)$, where individuals' decisions are influenced by their neighbors and the severity of the epidemic. In Section 2.2.2, we study $B_j(t)$ and analyze how the changes in individuals' health states may affect the change in $x_j(t)$.

2.2.1 Analysis of $D_j(t)$

Game theory models strategic interactions among agents, providing insights into decision-making across diverse scenarios, from social networks [35] to supply chains [36] and beyond. To model individuals' active behavior changes in response to their neighbors' impact and the proportion of infected individuals, we employ the evolutionary game theory, which is a useful framework to investigate the impact of neighbors on individuals' decisions [37,38]. The basic elements of the evolutionary game theory include individual, strategy, payoff, and strategy update rules. These elements will be introduced one by one in the following.

Individual and Strategy: Each individual is represented as a node in the information network. As mentioned in Section 2.1, we assume that there are a total of M possible protective behaviors $\{a_1, \cdots, a_M\}$ for susceptible individuals, and each behavior a_j corresponds to one strategy for a susceptible individual. For infected individuals, as mentioned in Section 2.1, they do not take any protective behavior such as home isolation to prevent the disease from spreading. Therefore, in this work, we focus on the analysis of susceptible individuals' behavior and study how their decisions are affected by their neighbors and the severity of the epidemic. In each time slot, m percent of susceptible individuals are randomly chosen as focal individuals. These focal individuals observe and imitate their neighbors' behaviors. The remaining susceptible individuals maintain their actions unchanged during this time slot.

The Payoff: In this paper, we study the protective behavior of susceptible individuals. Note that infected individuals have different health states from susceptible ones, and they adopt the same and fixed strategy of no protective behaviors. Therefore, in this work, we assume that susceptible individuals do not value these infected individuals' decisions, and the strategies of all susceptible individuals are only affected by their susceptible neighbors. So we define the payoff for susceptible individuals only, and ignore the payoffs of infected individuals, as they do not affect susceptible individuals' update of their strategies.

In each time slot, every susceptible individual receives a payoff determined by the chosen strategy and interactions with neighbors. In this paper, we consider two scenarios where the susceptible individual is rational and irrational. Therefore, we define the payoff of different behaviors based on the expected utility theory (EUT) [39] and prospect theory (PT) [23], respectively, where EUT models the individual as a rational person and PT considers the individual's irrationality. Here, following the prior work in [29], to simplify the analysis, we assume that either all individuals are rational or they are all irrational, and compare the two results to analyze the impact of users' irrationality on the co-evolution of individuals' behaviors and the epidemic.

Rational individuals' payoff function: Expected utility theory (EUT) is an economic theory that models the decision-making of rational individuals. When an individual chooses a specific behavior, denoted as a_j, it leads to L potential actual payoffs $o_{j,1}, o_{j,2}, ..., o_{j,L}$ with probabilities $p_{j,1}, p_{j,2}, ..., p_{j,L}$, respectively. It is worth noting that an individual may receive more than one actual payoff for their behavior, and $\sum_{k=1...L} p_{j,k} \neq 1$. For example, if an individual decides to go out for dinner during an epidemic, they will receive a positive payoff from enjoying the fine cuisine, while they may also face a negative payoff if they become infected. In addition, according to EUT, the perceived payoff may differ from the actual payoff. For example, the relationship between the perceived and actual payoffs is often not linear, and there is a phenomenon of diminishing marginal payoff [21]. In prior works in EUT, the value function $u^E(x)$ is used to model the relationship between the actual payoff x and the perceived payoff $u^E(x)$. Various forms of $u^E(x)$ have been used in the previous works, including the simplest form of $u^E(x) = x$, as well as the power function and the exponential function form [40]. Thus, in EUT, the payoff associated with adopting behavior a_j is calculated as the expected utility, which is denoted as U_j^{EUT} and is defined as:

$$U_j^{EUT} = \sum_{k=1...L} u^E(o_{j,k}) p_{j,k}. \tag{4}$$

In our behavior modeling and epidemic control problem, every susceptible individual adopting protective behavior a_j will obtain a fixed actual payoff of c_j, which is the payoff from the behavior itself, and the probability of obtaining this outcome is 1. One example is the gain from enjoying the fine cuisine of dining outside during an epidemic. If the individual is infected at the next moment, it will suffer from a loss of c_n with $c_n < 0$. For an individual adopting a_j, the probability of being infected at time t is approximately $\bar{k}\beta_j i(t)$ [41][1]. Therefore, in our model, the individual who takes a_j will obtain two potential actual payoffs. A payoff of c_j with probability 1, and a payoff of c_n with probability $\bar{k}\beta_j i(t)$. So the expected utility in (4) becomes

$$U_j^{EUT} = u^E(c_j) + u^E(c_n)\bar{k}\beta_j i(t). \tag{5}$$

Irrational individuals' payoff function: Different from the expected utility theory (EUT), the prospect theory (PT) considers the irrational tendencies exhibited by individuals when faced with uncertainty. In PT, individuals tend to overestimate the probability of small risks and underestimate the probability of large risks [21]. Therefore, not only are the actual and the perceived payoffs different, but the actual and the perceived probabilities are also different when irrational individuals face uncertainties.

Similar to EUT, the value function $u^P(x)$ in PT can take different forms, and one commonly used form is the power function [25]:

$$u^P(x) = \begin{cases} x^\sigma, & \text{if } x \geq 0, \\ -\lambda(-x)^\sigma, & \text{if } x < 0, \end{cases} \tag{6}$$

[1]We consider those epidemics with $\beta_j \ll 1$, such as SARS, MERS and common influenza [42–44], and we assume that $\bar{k}\beta_j < 1$.

where λ reflects the individual's sensitivity to gain and loss, and $\sigma \in (0, 1]$ reflects the curvature and shape of the value function. It is worth noting that the theoretical analysis in Sections 3 and 4 do not rely on the specific form of $u^P(x)$.

In addition, instead of using the actual probability p_j, individuals' perceived probability is $\omega(p_j, \alpha)$, where $\omega(p, \alpha)$ is the probability weighting function. Following the prior work in [22], in this work, we use the following weighting function to describe the relationship between the perceived probability $\omega(p, \alpha)$ and the actual probability p:

$$\omega(p, \alpha) = e^{(-(-lnp)^{\alpha})}, \ \ p \in [0, 1], \ \alpha \in (0, 1], \tag{7}$$

where α is the irrationality coefficient. A smaller α indicates that the individual is more irrational (or equivalently, less rational), and the difference between the actual and the perceived probabilities is larger. Note that when $\alpha = 1$, we have $\omega(p, 1) = p$, and the perceived and actual probabilities are the same. Meanwhile, from (7), we have $\omega(1, \alpha) = 1$ define $\omega(0, \alpha) = 0$. This ensures that $\omega(p, \alpha) \in [0, 1]$ and $\omega(p, \alpha)$ is an increasing function of p. For simplicity, we use the mean-field method and assume all individuals have the same α.

Given the probability weighting function in (7) and the value function $u^P(x)$, when an irrational individual chooses behavior a_j, which leads to L different potential payoffs $\{o_{j,k}\}$ with corresponding probabilities $\{p_{j,k}\}$, the expected payoff is

$$U_j^{PT} = \sum_{k=1...L} u^P(o_{j,k})\omega(p_{j,k}, \alpha). \tag{8}$$

In our problem, same as the analysis of U_j^{EUT} in the above, the individual who chooses behavior a_j will obtain two potential actual payoffs: a payoff of c_j with probability 1, and a payoff of c_n with probability $\bar{k}\beta_j i(t)$. So (8) can be expressed as

$$U_j^{PT} = u^P(c_n) \cdot \omega[\bar{k}\beta_j i(t), \alpha] + u^P(c_j). \tag{9}$$

Note that if the value functions of EUT and PT are identical (i.e., $u^E(x) = u^P(x)$) and the irrationality coefficient α is set to 1, then PT degenerates to EUT.

Strategy Update Rules: In each time unit, $mN_0(t)$ individuals are randomly selected as the focal individuals to update their strategies and others will keep their strategies unchanged, where m is the fraction of individuals who are chosen as the focal individuals, and $N_0(t)$ is the total number of susceptible individuals at time t in the network. The focal individuals tend to imitate their neighbors' behavior with a high payoff. Following the work in [45], given a focal individual v with strategy a_j and given v randomly chooses a neighbor z using strategy a_k, the probability the individual v changes its strategy to a_k is

$$p(a_j \to a_k) = \frac{1}{2} + \frac{w}{2}\frac{1}{U_{max}}(U_k - U_j), \tag{10}$$

where $w \in (0, 1]$ measures the strength of selection, and U_{max} is the normalization term to ensure $p(a_j \to a_k) \leq 1$. U_j and U_k are the payoffs of strategy a_j and a_k, respectively.

In our work, we assume that individuals with different behaviors are uniformly distributed in the entire network. Therefore, the probability that the focal individual v chooses behavior a_j is $x_j(t)$, which represents the proportion of susceptible individuals who choose behavior a_j at time t in the entire network. Meanwhile, the proportion of focal individual v's susceptible neighbors choosing behavior a_j is the same as the proportion of susceptible individuals choosing behavior a_j in the entire network.

Then the probability that $x_j(t)$ increases by $\dfrac{1}{N_0(t)}$ due to individuals' strategy change is

$$p\left(\Delta x_j = \frac{1}{N_0(t)}\right) = \sum_{l=1}^{M} x_j(t)x_l(t)p(a_l \to a_j), \tag{11}$$

where $N_0(t) = N_0 s(t)$ is the number of susceptible individuals at time t. Similarly, the probability that $x_j(t)$ decreases by $\dfrac{1}{N_0(t)}$ due to individuals' strategy change is

$$p\left(\Delta x_j = -\frac{1}{N_0(t)}\right) = \sum_{l=1}^{M} x_j(t)x_l(t)p(a_j \to a_l). \tag{12}$$

Combining (10) and (12), we have

$$\begin{aligned} D_j(t) =& mN_0(t)\left\{p\left(\Delta x_j = \frac{1}{N_0(t)}\right) \times \frac{1}{N_0(t)} - p\left(\Delta x_j = -\frac{1}{N_0(t)}\right) \times \frac{1}{N_0(t)}\right\} \\ =& \frac{mw}{U_{max}} \sum_{l=1}^{M} x_j(t)x_l(t)(U_j - U_l). \end{aligned} \tag{13}$$

2.2.2 *Analysis of $B_j(t)$*

In reality, even if individuals do not change their behaviors, the proportion of susceptible individuals with different behaviors will change over time due to transitions in health states. Let $s_j(t)$ be the fraction of individuals who are susceptible and adopt behavior a_j at time t among the entire population, that is, $s_j(t) = s(t)x_j(t)$, where $s(t)$ is the fraction of susceptible individuals among all users in the network, and $x_j(t)$ is the fraction of individuals adopting a_j among all the susceptible individuals. Note that $s(t) = \sum_{j=1}^{M} s_j(t)$, when all individuals do not change their behavior, we have

$$B_j(t) = \frac{d}{dt}\left(\frac{s_j(t)}{s(t)}\right) = \frac{d}{dt}\left(\frac{s_j(t)}{\sum_{l=1}^{M} s_l(t)}\right) = \frac{\sum_{l=1}^{M}[s_j'(t)s_l(t) - s_l'(t)s_j(t)]}{s^2(t)}. \tag{14}$$

Note that $s_j'(t)$, the first order derivative of $s_j(t)$, contains two parts. The first part represents the change caused by the infection of susceptible individuals, while the second part represents the change caused by the recovery of infected individuals. For the first part, as there are a total of $s_j(t)$ susceptible individuals adopting behavior a_j, and each of them has probability $\beta_j\bar{k}i(t)$ to be infected, we have $s_{j1}'(t) = -s_j(t)\beta_j\bar{k}i(t)$. For the second part, we assume that the recovered individuals would choose their behaviors based on the ratio of different behaviors of susceptible individuals in the network, similar to the work in [46]. Therefore, $\gamma i(t)$ infected individuals will recover, $x_j(t)$ of whom will choose action a_j, and we have $s_{j2}'(t) = \gamma x_j(t)i(t)$. By combining these two parts ($s_j'(t) = s_{j1}'(t) + s_{j2}'(t)$), we have

$$s_j'(t) = -s(t)x_j(t)\beta_j\bar{k}i(t) + \gamma x_j(t)i(t). \tag{15}$$

Given (14), (15) and $s_j(t) = s(t)x_j(t)$, we have

$$B_j(t) = \sum_{l=1}^{M} x_j(t)x_l(t)\bar{k}i(t)(\beta_l - \beta_j). \tag{16}$$

2.2.3 The Overall Behavior Change Dynamics

Combining (3), (13) and (16), the complete differential equations describing the dynamics of individual behavior change are

$$\frac{dx_j(t)}{dt} = \sum_{l=1}^{M} x_j(t)x_l(t)\bar{k}i(t)(\beta_l - \beta_j) + \frac{mw}{U_{max}} \sum_{l=1}^{M} x_j(t)x_l(t)(U_j - U_l),\ j = 1...M. \tag{17}$$

2.3 The Dynamics and the Steady States of the Epidemic-Behavior Co-Evolution Model

Based on the disease spread Eq. (2) and the behavior change dynamics (17), the M-choice epidemic-behavior co-evolution model is obtained as follows:

$$\frac{di}{dt} = i(t)(1 - i(t))\bar{\beta}\bar{k} - \gamma i(t),$$

$$\text{and } \frac{dx_j}{dt} = \sum_{l=1}^{M} x_j(t)x_l(t)\bar{k}i(t)(\beta_l - \beta_j) + \frac{mw}{U_{max}} \sum_{l=1}^{M} x_j(t)x_l(t)(U_j - U_l),\ j = 1...M. \tag{18}$$

Here, the first differential equation represents the dynamics of individuals' health states, and the subsequent M equations model the changes in the proportions of susceptible individuals choosing each of the M behaviors.

At the steady state, both the proportion of infected individuals $i(t)$ and the proportions of individuals adopting different behaviors $\{x_j(t)\}$ reach a stable state where there are no further changes in $i(t)$ and $\{x_j(t)\}$. Even if a small group of individuals becomes infected/recovered or changes their strategies, the steady state would be restored. We denote the steady state of the M-choice model as $(i^*, x_1^*, \cdots, x_{M-1}^*)$ with $x_M^* = 1 - \sum_{j=1}^{M-1} x_j^*$.

To find the steady state of our M-choice disease spread and behavior change model, we follow an approach that is similar to [46] and apply Lyapunov's first method [47].

Definition 1. The steady-state $(i^*, x_1^*, \cdots, x_{M-1}^*)$ satisfies: for $j = 1, \cdots, M-1$,

$$\left.\frac{di}{dt}\right|_{i=i^*} = 0,\ \left.\frac{dx_j}{dt}\right|_{x_j=x_j^*} = 0,\ Re(\lambda_k) < 0,\ k = 1, ..., M, \tag{19}$$

where $\{\lambda_k\}$ are the eigenvalues of the Jacobian matrix

$$\left.\begin{bmatrix} \frac{\partial i'}{\partial i} & \frac{\partial i'}{\partial x_1} & \cdots & \frac{\partial i'}{\partial x_{M-1}} \\ \frac{\partial x_1'}{\partial i} & \frac{\partial x_1'}{\partial x_1} & \cdots & \frac{\partial x_1'}{\partial x_{M-1}} \\ \vdots & \vdots & \ddots & \vdots \\ \frac{\partial x_{M-2}'}{\partial i} & \frac{\partial x_{M-2}'}{\partial x_1} & \cdots & \frac{\partial x_{M-2}'}{\partial x_{M-1}} \\ \frac{\partial x_{M-1}'}{\partial i} & \frac{\partial x_{M-1}'}{\partial x_1} & \cdots & \frac{\partial x_{M-1}'}{\partial x_{M-1}} \end{bmatrix}\right|_{(i^*, x_1^*, \cdots, x_{M-1}^*)}, \tag{20}$$

and $Re(x)$ represents the real part of x. As it is usually difficult to find the closed-form solution of (19), we often use numerical methods to find the steady states of the co-evolution of disease spread and behavioral choice.

3 Analysis of the Steady State and the Influence of Irrationality for the 2-Behavior Model

To obtain insights into the co-evolution process of epidemic spread and behavioral choice and their steady states, in this section, we consider a simple scenario where each susceptible individual can take two possible behaviors and the theoretical solution of (19) can be obtained. For example, a susceptible individual may either choose risky behavior such as continuing to go out in spite of the epidemic, or choose conservative behavior such as home isolation. Home isolation can significantly reduce the risk of being infected, but it leads to substantial economic loss and affects people's physical and mental well-being. During the epidemic, individuals need to choose between high-cost low-risk conservative behavior and low-cost high-risk risky behavior. Their decisions are often influenced by the severity of the epidemic and the potential loss due to home isolation. People tend to choose self-isolation when the epidemic poses a greater threat to their health, and they tend to go out when the loss due to home isolation is too high (e.g., losing their jobs and income). By investigating this simple scenario, this paper aims to gain insights into the co-evolution process and its steady states, and theoretically analyze the impact of irrationality on the epidemic as well as individuals' behaviors. For the more general scenario with more than two possible behavior choices, we use numerical solutions and simulation results to show the evolution process, and an example with three possible behavior choices is provided in Appendix A in Supplementary Material.

In this section, based on our model in the previous section, we analyze the evolution of the epidemic and the dynamics of individuals' choices between two behaviors: the risky behavior (going out) represented by a_1, and the conservative behavior (home isolation) represented by a_2. As an example, we assume that the infection rate for the risky behavior is β_1, while the infection rate for the conservative behavior is $\beta_2 = 0$ as isolation ensures no infection risk. Then we analyze the steady states when the individuals are all rational or irrational, respectively, and compare their results to investigate the influence of irrationality.

3.1 Steady State Analysis

3.1.1 The Steady States with All Rational Individuals

When all individuals are rational, the payoff is modeled by EUT in (5). Since $x_1(t) + x_2(t) = 1$, $x_2(t)$ can replaced by $1 - x_1(t)$. With two possible behavior choices and given the EUT payoff function (5), the differential equations in (18) can be expressed as:

$$\begin{cases} \dfrac{di}{dt} = \beta_1 \bar{k} i(t) x_1(t)(1 - i(t)) - \gamma i(t), \\ \dfrac{dx_1}{dt} = -\beta_1 \bar{k} x_1(t)(1 - x_1(t)) i(t) + k_0 x_1(t)(1 - x_1(t)) \cdot (u^E(c_1) + u^E(c_n)\beta_1 \bar{k} i(t) - u^E(c_2)), \end{cases} \tag{21}$$

where $k_0 = \frac{mw}{U_{max}} > 0$. To find the steady states of (21), we have the following Theorem 1.

Theorem 1. The steady state (i^E, x_1^E) of (21) satisfies (22),

$$(i^E, x_1^E) = \begin{cases} (0, 1), & \text{if } \bar{k} < \frac{\gamma}{\beta_1}, \\ \left(1 - \frac{\gamma}{\bar{k}\beta_1}, 1\right), & \text{if } \bar{k} > \frac{\gamma}{\beta_1}, \Phi_1 < 0, \\ \left(i^{(1)}, \frac{\gamma}{(1 - i^{(1)})\bar{k}\beta_1}\right), & \text{if } \bar{k} > \frac{\gamma}{\beta_1}, \Phi_1 \geq 0, \end{cases} \tag{22}$$

where $i^{(1)} = \frac{k_0(u^E(c_2) - u^E(c_1))}{(k_0 u^E(c_n) - 1)\bar{k}\beta_1}$, $\Phi_1 = -k_0(u^E(c_1) - u^E(c_2)) + (\gamma - \bar{k}\beta_1)(k_0 u^E(c_n) - 1)$.

When $\bar{k} = \frac{\gamma}{\beta_1}$, there is no steady state.

Proof: See Appendix B in Supplementary Material.

From Theorem 1, there are three possible steady states, which correspond to three different situations in reality:

- Case 1: The steady state $(0, 1)$ represents the extreme situation where the infection rate is too low and the epidemic will die out eventually even without any protection. So all individuals choose the risky behavior of going out. The evolution process reaches the steady state $(0, 1)$ when $\bar{k} < \frac{\gamma}{\beta_1}$, which is equivalent to $\frac{\beta_1}{\gamma} < \frac{1}{\bar{k}}$. The term $\frac{1}{\bar{k}}$ is the epidemic threshold of a homogeneous network [48]. If $\frac{\bar{\beta}}{\gamma} < \frac{1}{\bar{k}}$, the epidemic will die out; otherwise, it will spread out. Since $\bar{\beta} = \beta_1 x_1(t) \in [0, \beta_1]$, in this scenario, the epidemic will die out no matter which behavior individuals choose. Therefore, all individuals will choose the risky behavior in this steady state since it gives a higher payoff. Therefore, when $\bar{k} < \frac{\gamma}{\beta_1}$, the stable state is $i = 0$ and $x_1 = 1$.
- Case 2: For the steady state $\left(1 - \frac{\gamma}{\bar{k}\beta_1}, 1\right)$, two constraints need to be satisfied. The first constraint is $\bar{k} > \frac{\gamma}{\beta_1}$, which means that if all individuals choose the risky behavior, the epidemic will spread out. The second constraint is $\Phi_1 < 0$. To understand the second constraint, note that when all individuals choose the risky behavior with $x_1 = 1$, the proportion of infected individuals will reach the stable state $\hat{i} = 1 - \frac{\gamma}{\bar{k}\beta_1}$, which represents the maximum extent to which the epidemic can spread (proof: see Appendix C in Supplementary Material). If for all possible values of i in the range $[0, \hat{i}]$, we have $\frac{dx_1(t)}{dt} > 0$ for all $x_1(t) \in (0, 1)$,[2] then more individuals will choose the risky behavior over time, and ultimately all individuals will choose risky behavior at the steady state with $x_1 = 1$. This may happen when the payoff of risky behavior is much higher than that of the conservative behavior, with $c_1 \gg c_2$, or when the cost of being

[2]Note that from (21), if $x_1(t) = 0$ or 1, we have $\frac{dx_1(t)}{dt} = 0$.

infected c_n is very low. Note that from (21), $\frac{dx_1}{dt}|_{0\le i\le \hat{i},0<x_1<1} > 0$ is equivalent to $\Phi_1 < 0$, where Φ_1 is defined in (22). Therefore, when $\bar{k} > \frac{\gamma}{\beta_1}$ and $\Phi_1 < 0$, the steady state $\left(1-\frac{\gamma}{\bar{k}\beta_1},1\right)$ is reached, where all individuals choose the risk behavior, and the proportion of infected people reaches the maximum level $\hat{i}$.

- Case 3: The steady state $\left(i^{(1)},\frac{\gamma}{(1-i^{(1)})\bar{k}\beta_1}\right)$ represents the scenario other than the above two extreme cases. In this scenario, the epidemic will not die out, nor will it spread to the maximum extent, and at the steady state, $0 < i^{(1)} < \hat{i}$ of the individuals in the network will be infected. Meanwhile, $0 < \frac{\gamma}{(1-i^{(1)})\bar{k}\beta_1} < 1$ of susceptible individuals will choose the risky behavior. This happens when $\bar{k} > \frac{\gamma}{\beta_1}$ and $\Phi_1 \ge 0$.

3.1.2 The Steady States with Irrational Individuals

Next, we consider the scenario where all individuals are "irrational", and model their payoff function using the PT. By substituting the PT utility function (9) into (17), the dynamic of the epidemic and the behavior can be expressed as:

$$\begin{cases} \frac{di}{dt} = \beta_1\bar{k}i(t)x_1(t)(1-i(t)) - \gamma i(t), \\ \frac{dx_1}{dt} = -\beta_1\bar{k}x_1(t)(1-x_1(t))i(t) + k_0x_1(t)(1-x_1(t))\cdot(u^P(c_1)+u^P(c_n)\cdot\omega[\beta_1\bar{k}i(t),\alpha]-u^P(c_2)). \end{cases} \tag{23}$$

Similarly, we can get the steady state of (23) in Theorem 2.

Theorem 2. The steady state (i^P, x_1^P) of (23) satisfies:

$$(i^P,x_1^P) = \begin{cases} (0,1), & \text{if } \bar{k} < \frac{\gamma}{\beta_1}, \\ \left(1-\frac{\gamma}{\bar{k}\beta_1},1\right), & \text{if } \bar{k} > \frac{\gamma}{\beta_1}, \Phi_2 < 0, \\ \left(i^{(2)},\frac{\gamma}{(1-i^{(2)})\bar{k}\beta_1}\right), & \text{if } \bar{k} > \frac{\gamma}{\beta_1}, \Phi_2 \ge 0, \end{cases} \tag{24}$$

where $\Phi_2 = -k_0(u^P(c_1)-u^P(c_2)) - (\gamma-\bar{k}\beta_1) - k_0u^P(c_n)\cdot\omega[\bar{k}\beta_1-\gamma,\alpha]$,

and $i^{(2)}$ satisfies $k_0u^P(c_n)\cdot\omega[\bar{k}\beta_1 i^{(2)},\alpha] - \bar{k}\beta_1 i^{(2)} + k_0(u^P(c_1)-u^P(c_2)) = 0.$ (25)

When $\bar{k} = \frac{\gamma}{\beta_1}$, there is no steady state.

Proof: See Appendix D in Supplementary Material.

The three stable states in PT are similar to those in EUT:

- Case 1: The steady state (0,1) is the same as Case 1 under EUT. In this situation, the epidemic will always die out, and all individuals will choose the risky behavior.

- Case 2: The steady state $\left(1-\frac{\gamma}{\bar{k}\beta_1}, 1\right)$ is the same as Case 2 under EUT. In situations where the payoff for the risky behavior is extremely high or when the loss of being infected is very small, all individuals will choose risky behavior, causing the epidemic to spread to its maximum extent. Note that the first constraints in (22) and (24) are the same, while the second constraints are different as $\Phi_1 \neq \Phi_2$.
- Case 3: The steady state $\left(i^{(2)}, \frac{\gamma}{(1-i^{(2)})\bar{k}\beta_1}\right)$ is similar to Case 3 under EUT, where the epidemic does not extinct, nor does it spread to the maximum range.

3.2 Analysis of Individuals' Irrationality

In this section, we analyze the influence of individuals' irrationality on the steady state. In the weighting function in (7), the irrationality coefficient quantifies the irrationality degree of individuals, and a smaller value of α indicates that individuals are more irrational as the difference between the actual and perceived risk becomes larger. To analyze the impact of the irrationality coefficient on individuals' behavior, this paper compares the steady states (i^P, x_1^P) at different α, and we have the following Theorem 3.

Theorem 3. Given the same set of system parameters (β_1, γ, k_0, c_1, c_2, c_n and $\bar{k}$) and the same value function $u^P(x)$, let $0 < \underline{\alpha} < \bar{\alpha} < 1$ be two irrationality coefficients, and $(\bar{i}^P, \bar{x}_1^P)$ and $(\underline{i}^P, \underline{x}_1^P)$ are the steady states with $\bar{\alpha}$ and $\underline{\alpha}$, respectively, where the individuals with $\bar{\alpha}$ have low irrationality and individuals with $\underline{\alpha}$ have high irrationality. Then we have:

3a. When $\bar{k} < \frac{\gamma}{\beta_1}$, all individuals, regardless of their irrationality degrees, will choose risky behavior with $\bar{x}_1^P = \underline{x}_1^P = 1$, and the epidemic will eventually die out with $\bar{i}^P = \underline{i}^P = 0$.

3b. When $\bar{k} > \frac{\gamma}{\beta_1}$, $\Phi_2 \geq 0$ is not simultaneously satisfied for $\bar{\alpha}$ and $\underline{\alpha}$, we have the following conclusions.

If $1-\frac{\gamma}{\bar{k}\beta_1} \leq \frac{1}{\bar{k}\beta_1 e}$, there are two possibilities.

- When $\Phi_2 < 0$ for both $\bar{\alpha}$ and $\underline{\alpha}$, all individuals, regardless of their irrationality degrees, will choose risky behavior with $\bar{x}_1^P = \underline{x}_1^P = 1$.
- When $\Phi_2 < 0$ for $\bar{\alpha}$ and $\Phi_2 \geq 0$ for $\underline{\alpha}$, all individuals with low irrationality will choose the risky behavior with $\bar{x}_1^P = 1$. Meanwhile, only a subset of individuals with high irrationality will choose risky behavior with $\underline{x}_1^P < 1$.

On the contrary, if $1-\frac{\gamma}{\bar{k}\beta_1} \geq \frac{1}{\bar{k}\beta_1 e}$, there are two possibilities.

- When $\Phi_2 < 0$ for both $\bar{\alpha}$ and $\underline{\alpha}$, all individuals, regardless of their irrationality degree, will choose risky behavior with $\bar{x}_1^P = \underline{x}_1^P = 1$.
- When $\Phi_2 < 0$ for $\underline{\alpha}$ and $\Phi_2 \geq 0$ for $\bar{\alpha}$, all individuals with high irrationality will choose risky behavior with $\underline{x}_1^P = 1$. Meanwhile, only a subset of individuals with low irrationality will choose risky behavior with $\bar{x}_1^P < 1$.

3c. When $\bar{k} > \frac{\gamma}{\beta_1}$, $\Phi_2 \geq 0$ for both $\bar{\alpha}$ and $\underline{\alpha}$, the epidemic will neither die out nor spread to the maximum extent, and a fraction of individuals will choose the risky behavior at the steady state.

- In addition, if $\bar{i}^P \leq \frac{1}{\bar{k}\beta_1 e}$, we have $\bar{i}^P \geq \underline{i}^P, \bar{x}_1^P \geq \underline{x}_1^P$, i.e., compared to individuals with high irrationality, fewer individuals with low irrationality would choose the conservative behavior.
- On the contrary, if $\bar{i}^P \geq \frac{1}{\bar{k}\beta_1 e}$, we have $\bar{i}^P \leq \underline{i}^P, \bar{x}_1^P \leq \underline{x}_1^P$, i.e., compared to individuals with high irrationality, more individuals with low irrationality would choose the conservative behavior.

Proof: See Appendix E in Supplementary Material.

To better understand Theorem 3, note that in (24), Case 1 represents the situation where the infection rate is too low and the epidemic will eventually die out no matter how individuals choose their behaviors. Therefore, individuals' irrationality will not affect the outcome when $\bar{k} < \frac{\gamma}{\beta_1}$, as stated in Theorem 3a.

For Theorem 3b, when $\bar{k} > \frac{\gamma}{\beta_1}$ and $\Phi_2 \geq 0$ are not simultaneously satisfied for $\bar{\alpha}$ and $\underline{\alpha}$, if $1-\frac{\gamma}{\bar{k}\beta_1} \leq \frac{1}{\bar{k}\beta_1 e}$, the percentage of individuals with high irrationality choosing the risky behavior will be less than or equal to the percentage of individuals with low irrationality, i.e., $\underline{x}_1^P \leq \bar{x}_1^P$. This is because, in this scenario, the risk of being infected is low (i.e., $\bar{i}^P = \underline{i}^P = 1 - \frac{\gamma}{\bar{k}\beta_1} \leq \frac{1}{\bar{k}\beta_1 e}$), and higher irrationality makes individuals overestimate this small probability of risk, causing them to be more conservative. On the contrary, if $1-\frac{\gamma}{\bar{k}\beta_1} \geq \frac{1}{\bar{k}\beta_1 e}$, the percentage of individuals with high irrationality choosing the risky behavior will be larger than or equal to the percentage of individuals with low irrationality, i.e., $\underline{x}_1^P \geq \bar{x}_1^P$. This is because, in this scenario, the risk of being infected is high (i.e., $\bar{i}^P = \underline{i}^P = 1 - \frac{\gamma}{\bar{k}\beta_1} \geq \frac{1}{\bar{k}\beta_1 e}$), and higher irrationality makes individuals underestimate this large probability of risk, causing them to be more adventurous.

For Theorem 3c, when $\bar{k} > \frac{\gamma}{\beta_1}$ and $\Phi_2 \geq 0$ for both $\bar{\alpha}$ and $\underline{\alpha}$, both $(\bar{i}^P, \bar{x}_1^P)$ and $(\underline{i}^P, \underline{x}_1^P)$ belong to Case 3 in Theorem 2, where some individuals get infected while the rest do not. In this case, if the risk of getting infected is low when stable (i.e., $\bar{i}^P \leq \frac{1}{\bar{k}\beta_1 e}$), higher irrationality can motivate individuals to adopt conservative behaviors as they tend to overestimate this small risk, resulting in a decrease in the probability of being infected. On the contrary, if the risk of getting infected is high when stable (i.e., $\bar{i}^P \geq \frac{1}{\bar{k}\beta_1 e}$), higher irrationality can reduce individuals' cautiousness as they tend to underestimate this large risk, causing more people to be infected.

Note that from Section 2.2, if the value functions of EUT and PT are identical (i.e., $u^E(x) = u^P(x)$), then EUT can be considered as a special case of PT with $\alpha = 1$. Therefore, we can also apply Theorem 3 to make comparisons between rational individuals (following EUT) and irrational individuals (following PT).

In summary, irrationality tends to make individuals become more extreme, that is, risk-averse when the risk is small and risk-seeking when the risk is high.

4 Behavior Inducement to Control the Disease Spread

In this section, based on our previous analysis in Sections 2 and 3, we study how to guide individuals' behaviors and control epidemic spread through policy design and develop effective behavior inducement algorithms.

4.1 The Optimal Behavior Inducement Algorithms

We first discuss measures that governments can take to guide individuals' behaviors during an epidemic. For example, they can incentivize or penalize certain behaviors, such as subsidizing risky behaviors (e.g., going out) to boost the economy, penalizing risky behaviors, or encouraging conservative behaviors (such as staying at home and wearing masks) to control the disease spread. In our model, this means the parameters c_1 and c_2 can be changed. In addition, during an epidemic, individuals usually have different perceptions of the loss of being infected, which are largely due to the various propaganda efforts. So we assume that the parameter c_n can also be adjusted. Moreover, note that propaganda via social networks and media often affects individuals' irrationality [49], and thus, we assume that the irrationality coefficient α can be changed as well. In this work, to simplify the analysis, we consider the simple scenario where these parameters c_1, c_2, c_n, and α can be changed to the desired values. Our future work will consider a more practical scenario where the optimization parameters are the actions the government can take (such as rewarding or punishing specific behaviors through policies) instead of the exact values of these parameters.

Next, we discuss the goals of behavior guidance. The first goal is to control the spread of the disease at the steady state. For example, the government may wish to keep the number of infected people as low as possible. Here, the loss caused by the epidemic is represented as $l_1(i^P)$, where (i^P, x_1^P) is the steady state of PT. Also, if a large percentage of individuals choose conservative behavior such as self-isolation, it will significantly affect the economy and individuals' mental health. Therefore, the second loss term considered in our paper is the loss due to such conservative behavior $l_2(x_1^P)$. Furthermore, note that changing the values of c_1, c_2, c_n, and α through behavior inducements such as propaganda, subsidies, and penalties will incur costs. Therefore, the third goal is to minimize the cost associated with behavior guidance $l_3(\boldsymbol{\delta})$, where $\boldsymbol{\delta} = [\Delta\alpha, \Delta c_n, \Delta c_1, \Delta c_2]$ is the intervention vector quantifying the extent to which these variables are changed. Given c_1, c_2, c_n, and α before behavior guidance, the adjusted parameters are

$$\alpha' = \alpha + \Delta\alpha,\ c_n' = c_n + \Delta c_n,\ c_1' = c_1 + \Delta c_1,\ \text{and}\ c_2' = c_2 + \Delta c_2. \tag{26}$$

Since the irrationality coefficient should fall within (0, 1] and the payoff of being infected should be negative, we have $0 < \alpha + \Delta\alpha \leq 1$ and $c_n + \Delta c_n < 0$. The goal is to find the optimal $\boldsymbol{\delta}$ to minimize the total loss. The optimization problem is:

$$\begin{aligned} \min_{\boldsymbol{\delta}} \quad & l_1(i^P(\boldsymbol{\delta})) + l_2(x_1^P(\boldsymbol{\delta})) + l_3(\boldsymbol{\delta}) \\ s.t. \quad & 0 < \alpha + \Delta\alpha \leq 1, \\ & c_n + \Delta c_n < 0. \end{aligned} \tag{27}$$

In this work, we do not specify the specific forms of $l_1(i^P)$, $l_2(x_1^P)$, and $l_3(\boldsymbol{\delta})$, and they are assumed to be differentiable, i.e., $\frac{\partial l_1}{\partial i}$, $\frac{\partial l_2}{\partial x_1}$, and $\frac{\partial l_3}{\partial \boldsymbol{\delta}}$ exist. Moreover, we assume that $l_3(\boldsymbol{\delta})$ satisfies

$$\begin{cases} \frac{\partial l_3}{\partial \Delta\alpha} > 0 \quad \text{if} \ \ \Delta\alpha > 0, \\ \frac{\partial l_3}{\partial \Delta\alpha} < 0 \quad \text{if} \ \ \Delta\alpha < 0, \end{cases} \tag{28}$$

and the same constraint also holds for $\frac{\partial l_3}{\partial \Delta c_n}$, $\frac{\partial l_3}{\partial \Delta c_1}$ and $\frac{\partial l_3}{\partial \Delta c_2}$. This implies that compared to the case where no behavior guidance is taken with $\boldsymbol{\delta} = \mathbf{0}$, increasing or decreasing any of the variables (c_1, c_2, c_n, and α) will result in an increase in $l_3(\boldsymbol{\delta})$, and $l_3(\boldsymbol{\delta})$ has the minimum value at $\mathbf{0}$ with no behavior guidance.

From (24), there are three possible steady states. To solve the optimization problem (27), we need to consider all three possible steady states and analyze the optimal solution for each, which is very complicated. Then we introduce Theorem 4 to simplify this problem.

Given the system parameters and $\boldsymbol{\delta}$, let (i^0, x_1^0) and (i^P, x_1^P) be the steady states without and with behavior inducement, respectively. Let $\boldsymbol{\delta}^{(3)}$ be the optimal adjustment parameter when the steady state after adjustment (i^P, x_1^P) belongs to Case 3 in Theorem 2. That means

$$\begin{aligned} \boldsymbol{\delta}^{(3)} = \quad & \underset{\boldsymbol{\delta}}{argmin}\ l_1(i^P(\boldsymbol{\delta})) + l_2(x_1^P(\boldsymbol{\delta})) + l_3(\boldsymbol{\delta}) \\ s.t. \quad & 0 < \alpha + \Delta\alpha \le 1, \\ & c_n + \Delta c_n < 0, \\ & \bar{k} > \frac{\gamma}{\beta_1}, \Phi_2 \ge 0, \end{aligned} \tag{29}$$

where Φ_2 is defined in (24).

From our analysis in Appendix F in Supplementary Material, we have the following Theorem 4.

Theorem 4. For the optimization problem (27), if $l_3(\boldsymbol{\delta})$ satisfies (28), given $\boldsymbol{\delta}^{(3)}$ defined in (29), let (i^0, x_1^0) and (i^P, x_1^P) be the steady states without and with behavior guidance, respectively. Then the optimal solution of (27) is either $\mathbf{0}$ or $\boldsymbol{\delta}^{(3)}$. Specifically,

- if $i^0 = 0$ and $x_1^0 = 1$, i.e., the original steady state without behavior guidance belongs to Case 1 in (24), the optimal solution is $\mathbf{0}$. That means no behavior guidance is needed, and the objective function in (27) is minimized at $\mathbf{0}$.
- If $i^0 = 1 - \frac{\gamma}{\bar{k}\beta_1}$ and $x_1^0 = 1$, i.e., the original steady state belongs to Case 2 in (24), the optimal solution is either $\mathbf{0}$ or $\boldsymbol{\delta}^{(3)}$, and the optimal solution can be obtained by comparing $l_1(i^0) + l_2(x_1^0)$ with $l_1(i^P) + l_2(x_1^P) + l_3(\boldsymbol{\delta}^{(3)})$.
- If $0 < i^0 < 1 - \frac{\gamma}{\bar{k}\beta_1}$ and $0 < x_1^0 < 1$, i.e., the original steady state belongs to Case 3, the optimal solution is $\boldsymbol{\delta}^{(3)}$.

From Theorem 4, we only need to model and solve the problem for Case 3 in (24), which greatly reduces the complexity of our problem.

4.2 Solving the Optimization Problems

In this section, we consider the following scenario and use it as an example to demonstrate how to model and solve the optimization problem in (27). Consider the scenario where the government wants to control epidemic spread and reduce its impact on the economy and people's mental health. It means that, at the steady state after behavior inducement (i^P, x_1^P), the percentage of infected people i^P is no more than i_m, and the ratio of people choosing the risky behavior x_1^P is at least x_m. That is, there are two constraints $0 \le i^P \le i_m$ and $1 \ge x_1^P \ge x_m$. Here, we assume that $0 \le i_m \le 1$ and $0 \le x_m \le 1$.

Since the infection rate β_1, the recovery rate γ, and the average degree of the networks $\bar{k}$ are assumed to be fixed and cannot be changed, it is possible that there is no $\boldsymbol{\delta}$ that can make the steady-state (i^P, x_1^P) satisfy both constraints simultaneously. For example, from the analysis in Section 3, when the infection rate is very high, it is unlikely to control the epidemic to a very small range while everyone goes out without any protective measures. Therefore, given β_1, γ and $\bar{k}$, the first step is to determine if the two constraints $0 \le i^P \le i_m$ and $1 \ge x_1^P \ge x_m$ are feasible, i.e., whether it is possible to find $\boldsymbol{\delta}$ that make the steady state satisfy both constraints. Section 4.2.1 investigates how to determine the feasibility of the two constraints. If they are feasible, Section 4.2.2 explains the details of the optimization problem and proposes a fast algorithm to solve it. If they are not feasible, Section 4.2.3 investigates how to reformulate the problem and let the steady state (i^P, x_1^P) be as close as possible to the constraints.

4.2.1 The Feasibility Test

From Theorem 4, we only need to get the optimal solution in Case 3 and then we can get the optimal solution of the whole space by comparing it with $\mathbf{0}$. From (24), if the steady state (i^P, x_1^P) belongs to Case 3, it should satisfy

$$x_1^P = \frac{\gamma}{(1 - i^P)\bar{k}\beta_1}. \tag{30}$$

Note that in (30), x_1^P is an increasing function of i^P. Therefore, given $0 \le i^P \le i_m$, we have $x_1^P = \frac{\gamma}{(1 - i^P)\bar{k}\beta_1} \in [\frac{\gamma}{\bar{k}\beta_1}, \frac{\gamma}{(1 - i_m)\bar{k}\beta_1}]$. If $x_m \le \frac{\gamma}{(1 - i_m)\bar{k}\beta_1}$, then it is possible to find $\boldsymbol{\delta}$ whose corresponding steady-state (i^P, x_1^P) satisfies $0 \le i^P \le i_m$ and $1 \ge x_1^P \ge x_m$ simultaneously, and thus the two constraints are feasible. Otherwise, the two constraints are infeasible and cannot be satisfied at the same time.

Fig. 2 presents two examples of the feasible region of (i_m, x_m). The green area encompasses all (i_m, x_m) pairs where the constraints are feasible, while the red area comprises all infeasible constraints. If our behavior inducement algorithm attempts to reduce the infection proportion below i_m while increasing the proportion of individuals choosing risky behaviors above x_m, the point (i_m, x_m) should fall within the green area, i.e., satisfying $x_m \le \frac{\gamma}{(1 - i_m)\bar{k}\beta_1}$ for this goal to be feasible.

4.2.2 Solving the Optimization Problem with Feasible Constraints

If $0 \le i^P \le i_m$ and $1 \ge x_1^P \ge x_m$ are feasible, we discuss how to solve the optimization problem. Given the two constraints, we adopt the exterior-point method and transform the two constraints into a penalty function:

$$\boldsymbol{\mu}[P(i^P - i_m) + P(-i^P) + P(x_m - x_1^P) + P(x_1^P - 1)], \tag{31}$$

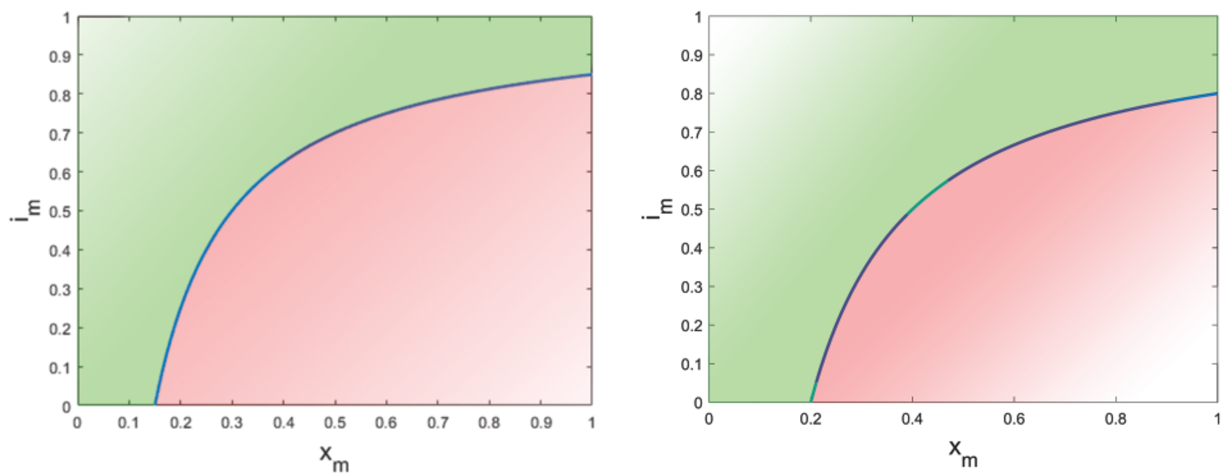

Figure 2: The range of i_m and x_m when (a) $\frac{\beta_1}{\gamma} = \frac{2}{3}$ (b) $\frac{\beta_1}{\gamma} = \frac{1}{2}$ with $\bar{k} = 10$. The green area represents the feasible constraints, and the red area represents the infeasible constraints

where $\boldsymbol{\mu}$ is a parameter that determines the intensity of the penalty, and $P(x) \triangleq (\max\{0, x\})^2$. We let $l_1(i^P) = \boldsymbol{\mu}[P(i^P - i_m) + P(-i^P)]$ and $l_2(x_1^P) = \boldsymbol{\mu}[P(x_m - x_1^P) + P(x_1^P - 1)]$, then the optimization problem (27) becomes:

$$\begin{aligned} &\min_{\boldsymbol{\delta}} \ \boldsymbol{\mu}[P(i^P - i_m) + P(-i^P) + P(x_m - x_1^P) + P(x_1^P - 1)] + l_3(\boldsymbol{\delta}), \\ &s.t. \quad 0 < \alpha + \Delta\alpha < 1, \quad ① \\ &\qquad\ \ c_n + \Delta c_n < 0. \quad ② \end{aligned} \tag{32}$$

According to Theorem 4, the optimization problem can be transformed into the problem in Case 3 and then we can get the optimal solution of the whole space by comparing it with **0**. Here we only consider the situation where $\bar{k} > \frac{\gamma}{\beta_1}$.[3] Then the optimization problem in Case 3 becomes:

$$\begin{aligned} &\min_{\boldsymbol{\delta}} \ \boldsymbol{\mu}[P(i^P - i_m) + P(-i^P) + P(x_m - x_1^P) + P(x_1^P - 1)] + l_3(\boldsymbol{\delta}), \\ &s.t. \quad 0 < \alpha + \Delta\alpha < 1, \quad ① \\ &\qquad\ \ c_n + \Delta c_n < 0, \quad ② \\ &\qquad\ \ (1 - i^P)\bar{k}\beta_1 x_1^P - \gamma = 0, \quad ③ \\ &\qquad\ \ k_0(u^P(c_1 + \Delta c_1) - u^P(c_2 + \Delta c_2)) + (\gamma - \bar{k}\beta_1) + k_0 u^P(c_n + \Delta c_n) \cdot \omega[\bar{k}\beta_1 - \gamma, \alpha + \Delta\alpha] \le 0, \quad ④ \\ &\qquad\ \ k_0 u^P(c_n + \Delta c_n) \cdot \omega[\bar{k}\beta_1 i^P, \alpha + \Delta\alpha] - \bar{k}\beta_1 i^P + k_0(u^P(c_1 + \Delta c_1) - u^P(c_2 + \Delta c_2)) = 0. \quad ⑤ \end{aligned} \tag{33}$$

[3] If $\bar{k} < \frac{\gamma}{\beta_1}$, the optimal solution is **0**, and no calculation is required. So we do not consider it in our work.

Here, $\omega[p, \alpha] = e^{(-(-lnp)^{\alpha})}$. Constraints ③, ④, and ⑤ guarantee that the steady state belongs to Case 3 in Theorem 2. The method for solving the problem is provided in Appendix G in Supplementary Material.

4.2.3 Reformulation of the Optimization Problem When the Constraints Are Infeasible

If the constraints $0 \le i^P \le i_m$ and $1 \ge x_1^P \ge x_m$ are not feasible, we reformulate the optimization problem and make (i^P, x_1^P) as close to (i_m, x_m) as possible. Specifically, we transform the two constraints $0 \le i^P \le i_m$ and $1 \ge x_1^P \ge x_m$ into $(i^P - i_m)^2 + (x_1^P - x_m)^2$ in the objective function, so that the steady-state (i^P, x_1^P) is close to (i_m, x_m) in the $i - x_1$ plane. Then the optimization problem (33) becomes

$$
\begin{aligned}
&\min_{\boldsymbol{\delta}} \; (i^P - i_m)^2 + (x_1^P - x_m)^2 + l_3(\boldsymbol{\delta}), \\
&s.t. \;\; 0 < \alpha + \Delta\alpha < 1, \\
&\quad c_n + \Delta c_n < 0, \\
&\quad (1 - i^P)\bar{k}\beta_1 x_1^P - \gamma = 0, \\
&\quad k_0(u^P(c_1 + \Delta c_1) - u^P(c_2 + \Delta c_2)) + (\gamma - \bar{k}\beta_1) + k_0 u^P(c_n + \Delta c_n) \cdot \omega[\bar{k}\beta_1 - \gamma, \alpha + \Delta\alpha] \le 0, \\
&\quad k_0 u^P(c_n + \Delta c_n) \cdot \omega[\bar{k}\beta_1 i^P, \alpha + \Delta\alpha] - \bar{k}\beta_1 i^P + k_0(u^P(c_1 + \Delta c_1) - u^P(c_2 + \Delta c_2)) = 0.
\end{aligned}
\tag{34}
$$

We can use the same method in Section 4.2.2 to solve (34), and the details are provided in Appendix H in Supplementary Material.

5 Simulation Results

In this section, we first run simulations to validate our steady state analysis of the co-evolution process and the effect of irrationality on individuals' behaviors and epidemic spread in Section 3. Then we validate the effectiveness of the behavior guidance algorithms proposed in Section 4. As there are few previous works have analyzed how to model irrational individuals in a pandemic, we do not compare our method with other works in this section.

5.1 Simulations of the Steady States of EUT and PT

Theorem 1 and Theorem 2 give theoretical analyses of the steady states when individuals are rational and irrational, respectively. To validate the two theorems, as an example, we conducted simulations on regular networks with 500 nodes. The physical contact network has a fixed degree of 10, while the information network has a degree of 20. We observe similar trends on other types of networks and with other parameters. We set the recovery rate to $\gamma = 0.03$ as an example and let the infection rate β_1 vary. We first run the simulation to validate the three cases of the steady state of EUT and PT. Since risky behaviors such as going out and not wearing a mask are the default behaviors most people take in their daily lives, we set $c_1 = 0$; conservative behaviors such as isolation and wearing masks can be regarded as behaviors with losses, so we set $c_2 < 0$. In this work, we let $c_1 = 0$, $c_2 = -1$, and $c_n = -20$. In order to facilitate the comparison between EUT and PT, we set $u^E(x) = u^P(x)$ and use the power function in (6) with $\sigma = 0.65$ and $\lambda = 1$ as an example. For other value functions, we observe the same trend and omit the results here. For each simulation setup, we repeat the experiment 50 times and show the average result below.

Fig. 3 shows the simulation and theoretical results of (i^E, x_1^E) and (i^P, x_1^P) with different infection rates β_1, where the theoretical results are calculated using Theorem 1 and Theorem 2. It can be seen that the simulation results match the theoretical results very well. The red area represents Case 1 in Theorem 1 and Theorem 2, wherein the infection rate is too low, resulting in no disease spread, then all individuals choose the risky behavior. Moving to the green area denoting Case 2 in Theorem 1 and Theorem 2, we observe a gradual rise in the proportion of infected individuals corresponding to an increasing infection rate. Despite this, as the infection rate is not high enough and the payoff for risky behavior remains high, individuals tend to choose risky behavior. Moving to the blue area denoting Case 3 in Theorem 1 and Theorem 2, the infection rate continues to increase, causing the payoff of the risky behavior to gradually decrease. Consequently, more individuals tend to choose conservative behavior, leading to a decline in the percentage of infected individuals.

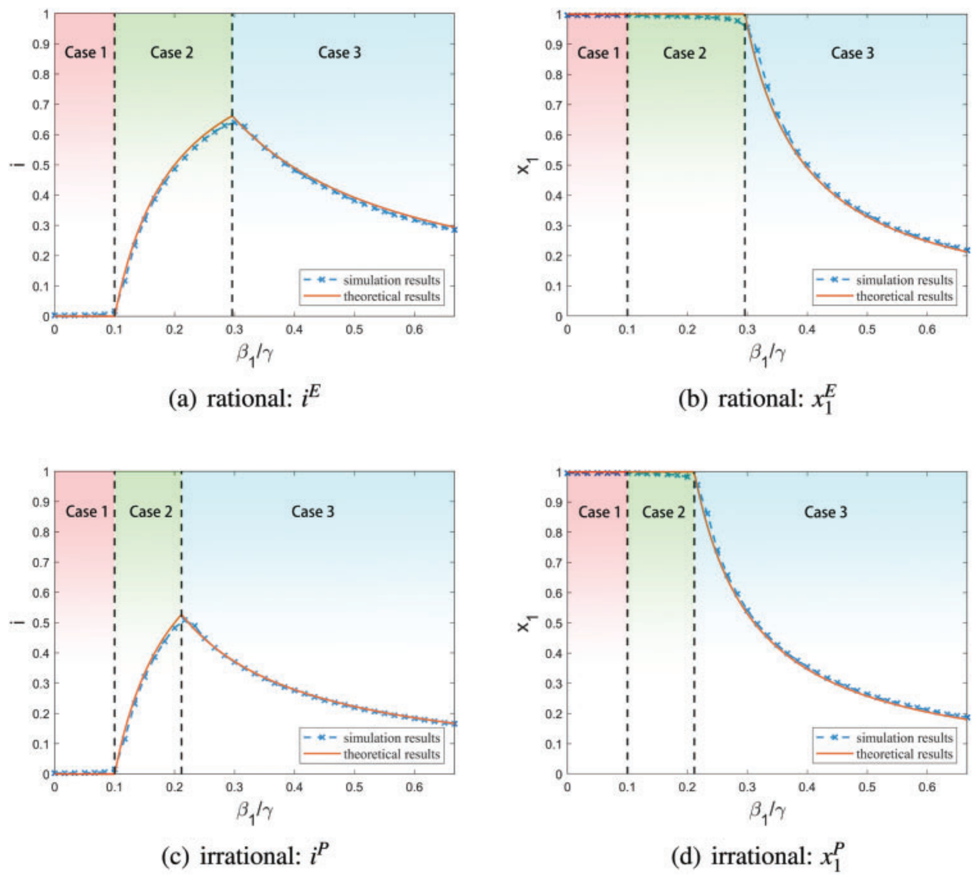

Figure 3: Simulation results of the steady states with rational and irrational individuals

Then we validate Theorem 3 and investigate the impact of irrationality on the steady states using the same simulation setup as before. Fig. 4 shows the average results of 50 simulation runs. We observe the same trend for other types of networks and other parameter settings. Note that in Fig. 4, $\alpha = 1$ (EUT) corresponds to the scenario with rational individuals, as explained in Section 2.2.1. In Fig. 4, as $\frac{\beta_1}{\gamma}$ increases, Point A is the boundary point separating Case 1 and Case 2, and Points B, C, and D are the boundary points separating Cases 2 and 3 with $\alpha = 0.6$, $\alpha = 0.8$, and $\alpha = 1$ (EUT), respectively. Then we analyze the results of $\alpha = 0.6$ and $\alpha = 0.8$ as an example. We use $(\underline{i}^P, \underline{x}_1^P)$ and $(\bar{i}^P, \bar{x}_1^P)$ to represent the steady states for $\alpha = 0.6$ and $\alpha = 0.8$. From Figs. 4a and 4b, we have:

- Before Point A, i.e., when $\frac{\beta_1}{\gamma} < \frac{1}{\bar{k}}$, irrationality does not influence individuals' behavior and the steady states in Case 1, as both curves with $\alpha = 0.6$ and $\alpha = 0.8$ have $\bar{x}_1^P = \underline{x}_1^P = 1$ and $\bar{i}^P = \underline{i}^P = 0$. Also, the boundary points separating Case 1 and Case 2 (Point A in Figs. 4a and 4b) are the same with different values of α. The results validate Theorem 3a.
- Between Points A and B, $\frac{\beta_1}{\gamma} > \frac{1}{\bar{k}}$, $\Phi_2 < 0$ for both $\alpha = 0.6, 0.8$. Therefore, from Theorem 3b, both individuals with low irrationality ($\alpha = 0.8$) and individuals with high irrationality ($\alpha = 0.6$) choose the risky behavior with $\underline{x}_1^P = \bar{x}_1^P = 1$ while the epidemic spreads to the maximum extent with $\underline{i}^P = \bar{i}^P = 1 - \frac{\gamma}{\bar{k}\beta_1}$, and this corresponds to Case 2 for both $(\underline{i}^P, \underline{x}_1^P)$ and $(\bar{i}^P, \bar{x}_1^P)$.
- Between Points B and C, $\frac{\beta_1}{\gamma} > \frac{1}{\bar{k}}$, $\Phi_2 < 0$ for $\alpha = 0.8$ but $\Phi_2 \geq 0$ for $\alpha = 0.6$. From Theorem 3b, all individuals with low irrationality still choose the risky behavior with the steady state $(\bar{i}^P = 1 - \frac{\gamma}{\bar{k}\beta_1}, \bar{x}_1^P = 1)$ in Case 2; while individuals with high irrationality are risk-averse with $\underline{x}_1^P < 1$, and $(\underline{i}^P, \underline{x}_1^P)$ belongs to Case 3.
- After Point C, $\frac{\beta_1}{\gamma} > \frac{1}{\bar{k}}$, $\Phi_2 \geq 0$ for both $\alpha = 0.8$ and $\alpha = 0.6$. From Theorem 2, both steady states for $\alpha = 0.8$ and $\alpha = 0.6$ belong to Case 3. Compared $(\underline{i}^P, \underline{x}_1^P)$ with $(\bar{i}^P, \bar{x}_1^P)$, as $\bar{i}^P \leq \frac{1}{\bar{k}\beta_1 e}$, from Theorem 3c, irrationality makes individuals risk-averse and more individuals with high irrationality choose conservative behaviors with $\underline{x}_1^P < \bar{x}_1^P$, and the epidemic spreads to a smaller range with $\underline{i}^P < \bar{i}^P$.

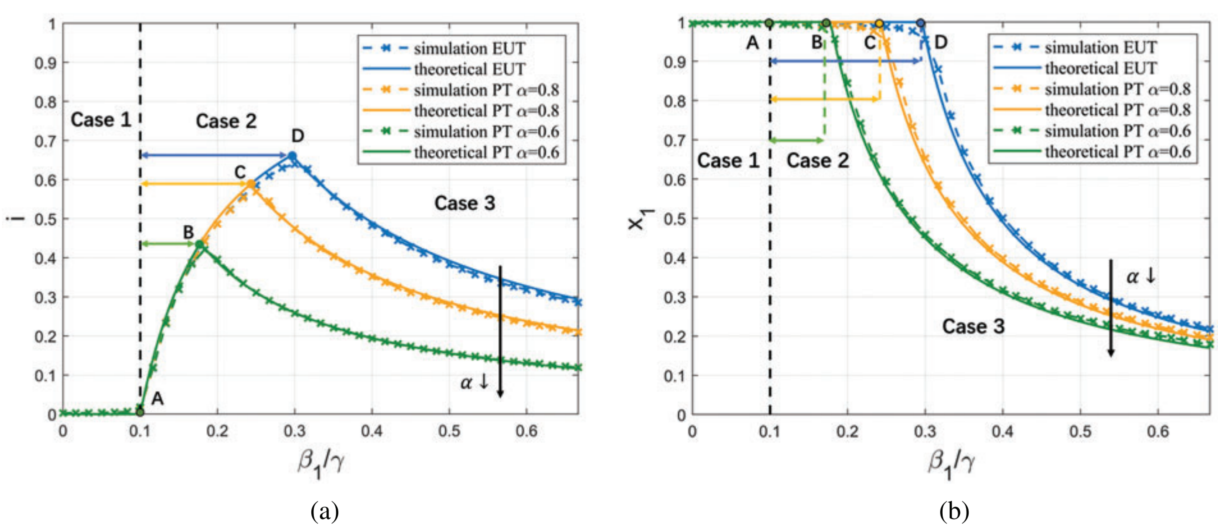

Figure 4: Simulation results of the steady states with different $\frac{\beta_1}{\gamma}$. (a) i^E and i^P (b) x_1^E and x_1^P

The above shows an example where irrationality promotes conservative behaviors, and in most parameter settings, irrationality makes individuals more conservative. Appendix I in Supplementary

Material shows an example where irrationality makes individuals risk-seeking. This situation only occurs when the infection rate is high, and the loss of disease is extremely low.

In summary, the simulation results effectively validate our analysis in Theorem 3.

5.2 Simulations of the Behavior Inducement Algorithm

Then we simulate the behavior inducement algorithm proposed in Section 4. We run simulations on regular networks with 500 nodes and a fixed degree of 10 for both the physical contact network and the information network. We let $c_1 = 0.5$, $c_2 = -1$, $c_n = -10$, $\gamma = 0.03$ and $\beta_1 = 0.01, 0.02$. For the loss term $l_3(\boldsymbol{\delta})$, we use the simple 2-norm $l_3(\boldsymbol{\delta}) = \|\boldsymbol{\delta}\|_2^2$ as an example, and observe similar trends for other loss functions. We conducted simulations to validate the behavior inducement algorithm under feasible and infeasible constraints, respectively. The corresponding results are illustrated in Figs. 5 and 6. Additionally, the loss function value of the algorithm is shown in Fig. 7.

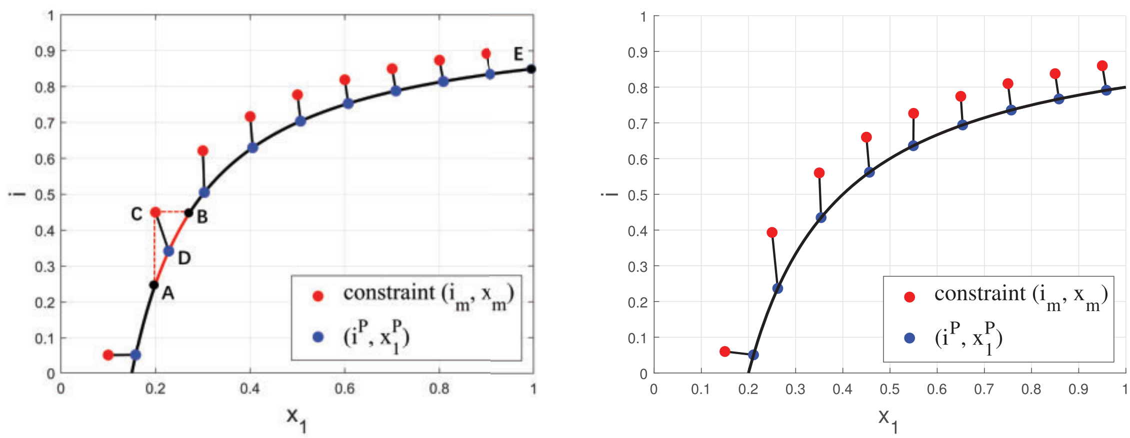

(a) $\frac{\beta_1}{\gamma} = \frac{2}{3}$ (b) $\frac{\beta_1}{\gamma} = \frac{1}{2}$

Figure 5: Simulation results of behavior inducement algorithm with feasible constraints (i_m, x_m)

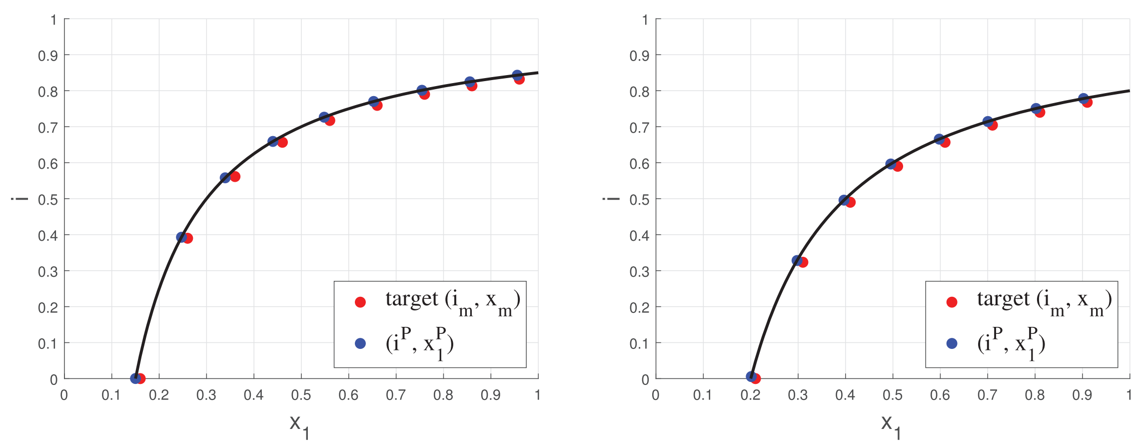

(a) $\frac{\beta_1}{\gamma} = \frac{2}{3}$ (b) $\frac{\beta_1}{\gamma} = \frac{1}{2}$

Figure 6: Simulation results of the behavior inducement algorithm with infeasible constraints (i_m, x_m)

The results of the proposed algorithm under feasible constraints are shown in Fig. 5. The black solid line represents the boundary between the feasible and infeasible regions; (i_m, x_m) above this line are feasible constraints where it is possible to find $\boldsymbol{\delta}$ to satisfy $0 \le i^P \le i_m$ and $1 \ge x_1^P \ge x_m$, and (i_m, x_m) below this line are infeasible. Moreover, since β_1, γ, and $\bar{k}$ are fixed, the black solid line includes all possible (i^P, x_1^P), where point E represents Case 2 and the other points in the black solid line represent Case 3. The red dots represent the limits (i_m, x_m) we set in our simulations, and it can be seen that they are all feasible. The blue dots show the steady states after using the proposed behavior guidance algorithm in Section 4.2.2, and they all satisfy $0 \le i^P \le i_m$ and $1 \ge x_1^P \ge x_m$. Using the constraint (i_m, x_m) labeled as **Point C** in Fig. 5a, the steady state (i^P, x_1^P) should fall within the range from point A to point B to satisfy the constraints $0 \le i^P \le i_m$ and $1 \ge x_1^P \ge x_m$, and the proposed behavior guidance algorithm selects **Point D** in this range to minimize the loss function in (33). The values of the loss function in (33) at each iteration are shown in Fig. 7a. As shown there, the loss function value decreases after each iteration and converges after 10,000 iterations. From Figs. 5 and 7a, under feasible constraints, our behavior inducement algorithm gets great results and converges well.

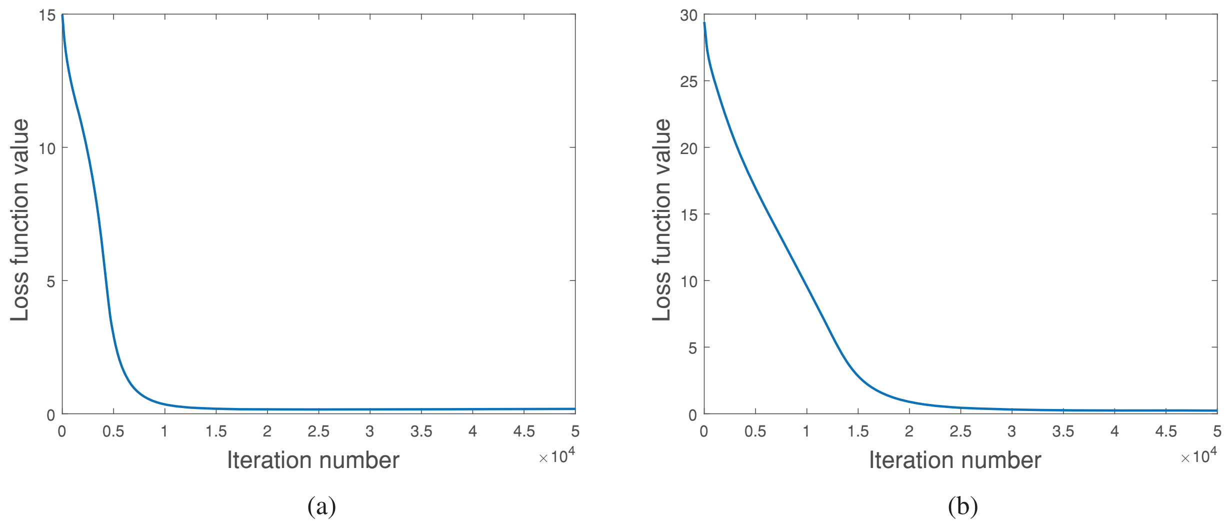

Figure 7: Simulation results of the behavior inducement algorithms. (a) The loss function in (33) with feasible constraints, and (b) the loss function in (34) with infeasible constraints

Simulation results of the proposed behavior inducement algorithm with infeasible constraints are shown in Fig. 6. Here, the given two constraints (i_m, x_m) are below the boundary of the feasible region and impossible to satisfy at the same time. It can be seen that although the steady state with behavior guidance cannot satisfy the two constraints simultaneously, it is on the boundary of the feasible region and very close to (i_m, x_m). The value of the loss function in (34) after each iteration is shown in Fig. 7b, where it decreases and converges as the number of iterations increases. From Figs. 6 and 7b, under infeasible constraints, our behavior inducement algorithm successfully moves the steady state closer to (i_m, x_m) with good convergence.

In summary, from Fig. 5–7, our behavior inducement algorithm is effective and converges well.

6 Real User Tests

While the simulation experiments have validated our theoretical analysis, it is necessary to further validate our conclusions using real user tests. However, obtaining real user data on behavioral choices, network structure, and spread data simultaneously poses a significant challenge. Therefore, we qualitatively validate our conclusions through sociological experiments. In our test, 550 subjects were interviewed, including 237 males and 313 females. The distribution of data is provided in Appendix J in Supplementary Material.

In our test, we first collect data to estimate the irrationality coefficient α of the subjects. Note that in Sections 2 and 3, to simplify the analysis, we assume that all individuals have the same value of α, which can be considered as the average value of α over the entire network. In reality, the irrationality coefficient α varies from person to person. Therefore, in our test, we estimate α for each individual separately. Next, we gather data on the subjects' behavioral choices in various scenarios during a pandemic. This data collection process allows us to capture individuals' risk preferences. Finally, we analyze the relationship between the irrationality coefficient α and the risk preference. By examining this relationship, we gain insights into how individuals' irrationality impacts their decisions during an epidemic and validate our analysis in Section 3.

6.1 Estimating the Irrationality Coefficient α

Data collection: Following the works in [23–25], we estimate the subjects' irrationality coefficient α in a way similar to gambling games. In our experiments, subjects are presented with a scenario where they have a probability p_i of suffering from a large financial loss. However, they are also given the option to purchase insurance at different prices to mitigate the potential loss. Then, the subjects are asked to make a decision regarding whether they would choose to buy the insurance. Below is an example we use in our experiment.

Question A: You have a 10% *probability of losing ¥100, but if you choose to buy insurance, it can be guaranteed that you will avoid this loss. Then, what is the insurance price you can accept?*

a. When the price is lower than ¥10, I will buy the insurance.

b. When the price is lower than ¥20 but higher than ¥10, I will buy the insurance.

c. When the price is lower than ¥30 but higher than ¥20, I will buy the insurance.

d. When the price is lower than ¥40 but higher than ¥30, I will buy the insurance.

e. When the price is lower than ¥50 but higher than ¥40, I will buy the insurance.

f. Even if the price is higher than ¥50, I will buy the insurance.

After the subjects have made their initial choices, a refined set of choices is presented to them to obtain fine-grained results. For instance, if a subject chooses option *c* in the above question, the prices shown in the subsequent question will be narrowed down to a range between ¥30 and ¥40, such as {¥30–¥32, ¥32–¥34, ¥34–¥36, ¥36–¥38, ¥38–¥40}. This process continues until the range is narrowed down to ¥1. For each subject, we change the probability p_i in the questionnaire, repeat the above process, and get multiple pairs of (p_i, r_i), where r_i is the final acceptable insurance price of the subject.

Estimation of α: If the subject chooses an acceptable insurance price of r_i to avoid the loss of ¥100 with probability p_i, then for this subject, a loss of ¥100 with probability p_i is equivalent to a loss of r_i with probability 1. Then from (8), we have:

$$\omega(p_i, \alpha)u^P(-100) + \omega(1 - p_i, \alpha)u^P(0) = \omega(1, \alpha)u^P(-r_i). \tag{35}$$

Similar to [25], we use (7) and (6) as the probability weighting function and the value function, respectively, in our work. Note that from the definitions, we have $u^P(0) = 0$ and $\omega(0, \alpha) = 0$, then we have:

$$- e^{(-(-lnp_i)^{\alpha})}\lambda(100)^{\sigma} = -\lambda(r_i)^{\sigma}, \tag{36}$$

which is equivalent to

$$ln\left(-ln\left(\frac{r_i}{100}\right)\right) = \alpha ln(-ln(p_i)) - ln(\sigma). \tag{37}$$

In (37), $ln\left(-ln\left(\frac{r_i}{100}\right)\right)$ is a linear function of $ln(-ln(p_i))$. We set $\sigma = 0.65$ following the work in [25]. Given the collected pairs $\{(p_i, r_i)\}$ from one subject, we use linear regression to find α in (37) for this subject.

6.2 Measuring Individuals' Risk Preference

Data Collection: Then we proceed to collect data on the behavioral choices of different subjects when confronted with risky scenarios during a pandemic. In each question of this section, subjects are presented with a specific epidemic situation. Within each scenario, subjects must choose between going out and staying at home. They are informed that if they choose to go out, there is a certain probability of becoming infected. If they decide to stay at home, they are guaranteed not to be infected, but they will suffer from some form of loss. Below is an example in our experiment.

Question B: There is an epidemic spreading right now. If you come into contact with an infected person, you have a 5% probability of being infected. If you choose to go out, you will be in close contact with 20 people every day. If you decide to stay at home, you are guaranteed not infected but will suffer from some losses. However, if you go out, there is a chance of becoming infected. The loss of being infected is 20 times that of the loss due to home isolation. Your city has a population of 1 million, then:

a. When there is no confirmed case in the city, I will go out.

b. When the number of confirmed cases in the city is less than 10, I will go out.

c. When the number of confirmed cases in the city is less than 100, I will go out.

d. When the number of confirmed cases in the city is less than 1,000, I will go out.

e. When the number of confirmed cases in the city is less than 10,000, I will go out.

f. When the number of confirmed cases in the city is less than 100,000, I will go out.

g. When the number of confirmed cases in the city is higher than 100,000, I will still go out.

Calculating Individuals' Risk Preference I_x: We use the risk preference I_x to reflect the behavioral tendencies of the subjects. The risk preference I_x for each individual corresponds to the proportion of times choosing the risky behavior in various scenarios in the questionnaire. This indicator ranges between 0 and 1, where values closer to 1 indicate a more risky behavioral tendency. It is important to note that in our model, x_1^P denotes the proportion of individuals choosing the risky behavior. A higher I_x value within a group implies a greater inclination of individuals towards risky behavior, resulting in a higher x_1^P value. Then we analyze the relationship between irrationality and behavioral choice.

6.3 Analysis of the Relationship between Irrationality and Behavioral Choice

We classify subjects into different groups based on their irrationality coefficient α, with the aim of grouping together individuals who share similar values of α within each respective group. We calculate the mean value of I_x and analyze the relationship between α and I_x. The results are illustrated in Fig. 8a. We can see that groups with a smaller α (i.e., a higher degree of irrationality) also have a smaller average risk preference I_x, which is consistent with our conclusion. The Spearman coefficient of α and average I_x in different groups is 1.00 ($p < 0.01$), which means α and I_x have a strong correlation. In our theoretical analysis and simulations, we find that irrationality makes more conservative in most parameter settings, and irrationality makes individuals more risk-seeking only occurs when the infection rate is high, and the loss of disease is extremely low. Since the parameter settings of our real user tests do not meet this condition, irrationality causes individuals to be more conservative. The results of real user tests are consistent with the theoretical analysis.

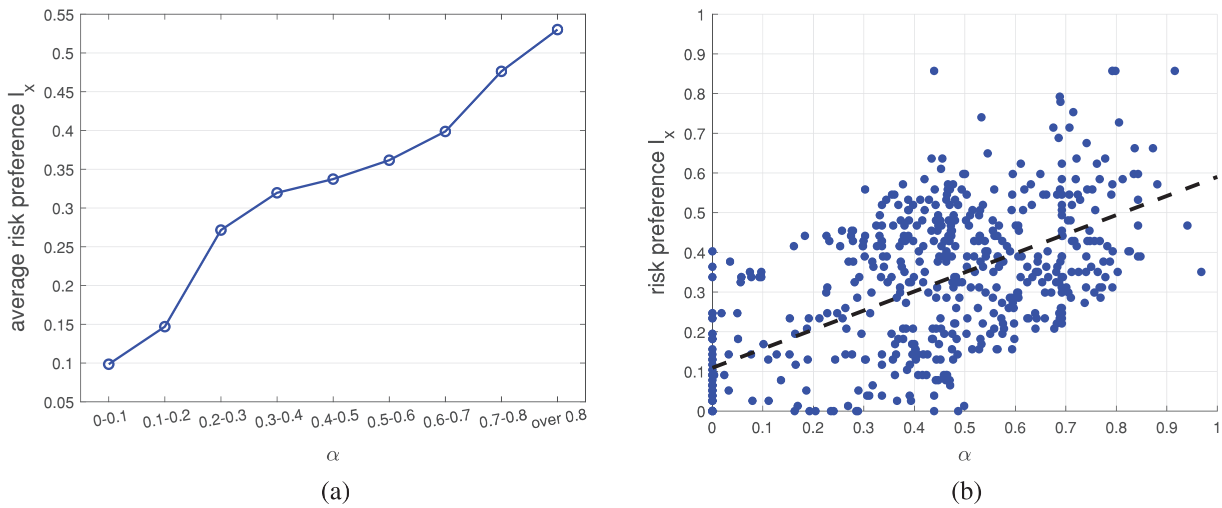

Figure 8: (a) The relationship between α and average risk preference I_x. (b) The scatter plot of α and risk preference I_x. The dashed line shows regression estimates

Moreover, we also plot scatter plots of α and I_x for all samples, as shown in Fig. 8b. It can be seen that there is a certain correlation between the two. The Pearson correlation coefficient of α and I_x of each sample is 0.619 ($p < 0.001$), indicating a strong correlation between the two [50,51]. This indicates that irrationality causes individuals to be more conservative, which is consistent with our conclusion.

7 Discussion

7.1 The Impact of Cultural and Social Elements

Cultural and social elements can influence individual behavioral choices and disease spread, and our model can be used to analyze them to a certain extent.

First, in reality, an individual's understanding and views of an epidemic may be affected by culture, beliefs, and social environment. For example, people in different countries have different opinions about COVID-19 [52]. Moreover, political opinions will also affect individuals' concerns about COVID-19 [53]. In our model, people with different cultures and political opinions can have different c_n and α. That is, they have different perceptions of the losses caused by the epidemic and may have different degrees of irrationality. Therefore, our model can be used to analyze the impact of culture, political opinions, social elements, etc., on individual behavioral choices and epidemic spread.

In addition, different costs of implementing policies in different cultures and countries can be reflected in our behavior inducement algorithm. For example, in some countries or cultures, the cost of implementing policies is lower, and individuals are more inclined to obey behavioral inducement. In our model, that means they have a lower $l_3(\boldsymbol{\delta})$. Therefore, our behavior inducement method can also analyze the effects of government guidance in different cultures and countries.

7.2 The Implementation of Behavior Inducement Method

In Section 4, we discuss how to control the spread of disease through behavior inducement. We assume that individuals' c_n, c_1, c_2 and α can be changed, here we discuss how to implement the behavior inducement method.

Change people's understanding of the diseases: Propaganda can influence people's awareness of the dangers of diseases. For example, during the COVID-19 crisis, there was a tendency among supporters of the US Democratic Party to perceive COVID-19 as more harmful compared to supporters of the Republican Party. This disparity largely stemmed from the propaganda policies employed by the two parties [53]. Therefore, individuals' c_n can be changed by propaganda.

Reward or punish specific behaviors: Governments can guide people's behavior by rewarding and punishing specific behaviors. For example, reward the behavior of staying at home or punish the behavior of going out to control the spread of the disease. In this approach, an individual's c_1 and c_2 can be changed.

Change people's irrationality coefficient: Propaganda via social networks and media can influence individuals' irrationality [49]. For example, the government can publicize during the disease that people do not need to overestimate the probability of small events and do not need to panic too much, which could reduce the irrationality of individuals. Then individuals' α can be changed.

7.3 Guidelines

Through theoretical analysis and experiments, we get some insights into disease spread control, which can guide government policies to a certain extent.

First, considering the practicalities of governance, the government can employ a multifaceted approach to control spread, utilizing methods like incentivizing and penalizing behaviors and raising awareness about the disease through propaganda. Through our experiments, we observe that the efficacy of a singular measure diminishes as its intensity increases. Therefore, employing multiple measures simultaneously can yield superior outcomes at a reduced cost.

Second, the influence of irrationality has great significance. The degree of individual irrationality can be affected by propaganda and other means. Through experiments, we find that changing the irrational coefficient α can effectively affect individual behavioral choices and disease spread. In reality, this provides a new approach to controlling the spread of disease by influencing the irrational degree of individuals.

Finally, as discussed in Section 4.2, there are limits to the two goals of controlling spread and reducing economic losses. Therefore, governments need to formulate reasonable policies and make a trade-off between controlling the spread of disease and reducing economic losses. For example, in the case of certain seasonal and highly detrimental diseases, the government may opt to maximize control measures to limit the spread, even if it will lead to substantial short-term economic losses. In the case of prolonged epidemic diseases, it becomes crucial to pay increased attention to the long-term economic loss.

8 Conclusion

In this paper, we propose an epidemic-behavior co-evolution framework to analyze the co-evolution of user behavior and the disease spread during an epidemic. Our model considers the irrationality of individuals' decision-making processes, and our theoretical analysis shows that individual irrationality polarizes individual behavior choices. That is, irrationality makes users risk-averse when the probability of being infected is small, while they tend to be risk-seeking when the probability of being infected is large. We then propose a behavior inducement algorithm to control the disease spread and reduce losses by guiding individual behavior. Simulation results show the correctness of our theoretical analysis and verify the validity of our guidance control method. We also qualitatively prove the correctness of our conclusions using real-user tests. Different from the prior works, in this work, we use prospect theory to model the individuals' irrational behaviors during an epidemic and the co-evolution of individuals' behaviors and the epidemic. Our research contributes to comprehending the irrational behavioral choices made by individuals during epidemics. Additionally, our behavior inducement approach does not rely on mandatory policies like prior works, providing a viable framework for governments to effectively control disease spread during epidemics.

Acknowledgement: None.

Funding Statement: The authors received no specific funding for this study.

Author Contributions: Wenxiang Dong built the model, derived the theory, conducted simulations and real user tests, and wrote the paper. H. Vicky Zhao provided research guidance and edited the paper.

Availability of Data and Materials: In our ethics application for the real user tests, we promised to protect the privacy of all test subjects. Therefore, we cannot provide the specific data of each sample in the real user tests. The distribution of the data can be provided upon request.

Conflicts of Interest: The authors declare that they have no conflicts of interest to report regarding the present study.

Supplementary Materials: The supplementary material is available online at https://doi.org/10.32604/cmes.2024.047156.

References

1. Wang, Y., Chakrabarti, D., Wang, C., Faloutsos, C. (2003). Epidemic spreading in real networks: An eigenvalue viewpoint. *22nd International Symposium on Reliable Distributed Systems*, Florence, Italy, IEEE.
2. Tong, H., Prakash, B. A., Tsourakakis, C., Eliassi-Rad, T., Faloutsos, C. et al. (2010). On the vulnerability of large graphs. *2010 IEEE International Conference on Data Mining*, Sydney, Australia, IEEE.
3. Chen, C., Tong, H., Prakash, B. A., Tsourakakis, C. E., Eliassi-Rad, T. et al. (2015). Node immunization on large graphs: Theory and algorithms. *IEEE Transactions on Knowledge and Data Engineering, 28(1),* 113–126.
4. Ahmad, M., Tariq, J., Shabbir, M., Khan, I. (2017). Spectral methods for immunization of large networks. *Australasian Journal of Information Systems, 21,* 1563.
5. Saxena, C., Doja, M., Ahmad, T. (2018). Group based centrality for immunization of complex networks. *Physica A: Statistical Mechanics and its Applications, 508,* 35–47.
6. Birge, J. R., Candogan, O., Feng, Y. (2022). Controlling epidemic spread: Reducing economic losses with targeted closures. *Management Science, 68(5),* 3175–3195.

7. Wan, R., Zhang, X., Song, R. (2021). Multi-objective model-based reinforcement learning for infectious disease control. *Proceedings of the 27th ACM SIGKDD Conference on Knowledge Discovery & Data Mining*, New York, USA, ACM.
8. Hota, A., Godbole, J., Pare, P. (2021). A closed-loop framework for inference, prediction, and control of sir epidemics on networks. *IEEE Transactions on Network Science and Engineering, 8(3),* 2262–2278.
9. Alazman, I., Albalawi, K. S., Goswami, P., Malik, K. (2023). A restricted sir model with vaccination effect for the epidemic outbreaks concerning COVID-19. *Computer Modeling in Engineering & Sciences, 137(3),* 841–854. https://doi.org/10.32604/cmes.2023.028674
10. Chen, Z., Zha, H., Shu, Z., Ye, J., Pan, J. (2022). Assess medical screening and isolation measures based on numerical method for COVID-19 epidemic model in japan. *Computer Modeling in Engineering & Sciences, 130(2),* 841–854. https://doi.org/10.32604/cmes.2022.017574
11. Farman, M., Akgül, A., Ahmad, A., Baleanu, D., Umer Saleem, M. (2021). Dynamical transmission of coronavirus model with analysis and simulation. *Computer Modeling in Engineering & Sciences, 127(2),* 753–769. https://doi.org/10.32604/cmes.2021.014882
12. Chu, Y. M., Sultana, S., Rashid, S., Alharthi, M. S. (2023). Dynamical analysis of the stochastic COVID-19 model using piecewise differential equation technique. *Computer Modeling in Engineering & Sciences, 137(3),* 2427–2464.
13. Xu, Y. H., Wang, H. J., Lu, Z. W., Hu, M. B. (2023). Impact of awareness dissemination on epidemic reaction–diffusion in multiplex networks. *Physica A: Statistical Mechanics and its Applications, 621,* 128723.
14. Zhang, H. F., Xie, J. R., Tang, M., Lai, Y. C. (2014). Suppression of epidemic spreading in complex networks by local information based behavioral responses. *Chaos, 24(4),* 043106.
15. Wu, Q., Fu, X., Small, M., Xu, X. J. (2012). The impact of awareness on epidemic spreading in networks. *Chaos, 22(1),* 013101.
16. Bagnoli, F., Lio, P., Sguanci, L. (2007). Risk perception in epidemic modeling. *Physical Review E, 76(6),* 061904.
17. Shang, Y. (2013). Modeling epidemic spread with awareness and heterogeneous transmission rates in networks. *Journal of Biological Physics, 39(3),* 489–500.
18. Funka, S., Gilada, E., Watkinsb, C., Jansena, V. A. (2009). The spread of awareness and its impact on epidemic outbreaks. *Proceedings of the National Academy of Sciences of the United States of America, 106(16),* 6872–6877.
19. Granell, C., Gómez, S., Arenas, A. (2013). Dynamical interplay between awareness and epidemic spreading in multiplex networks. *Physical Review Letters, 111(12),* 128701.
20. Granell, C., Gómez, S., Arenas, A. (2014). Competing spreading processes on multiplex networks: Awareness and epidemics. *Physical Review E, 90(1),* 012808.
21. Kahneman, D., Tversky, A. (2013). Prospect theory: An analysis of decision under risk. In: *Handbook of the fundamentals of financial decision making: Part I*, pp. 99–127. Hackensack, NJ, USA: World Scientific.
22. Prelec, D. (1998). The probability weighting function. *Econometrica, 66(3),* 497–527.
23. Tversky, A., Kahneman, D. (1992). Advances in prospect theory: Cumulative representation of uncertainty. *Journal of Risk and Uncertainty, 5(4),* 297–323.
24. Gonzalez, R., Wu, G. (1999). On the shape of the probability weighting function. *Cognitive Psychology, 38(1),* 129–166.
25. Prelec, D. (2000). *Compound invariant weighting functions in prospect theory*, pp. 67–92. Cambridge, UK: Cambridge University Press Cambridge.
26. Ji, Y., Ma, Y. (2023). The robust maximum expert consensus model with risk aversion. *Information Fusion,* 101866.
27. Oraby, T., Bauch, C. T. (2015). Bounded rationality alters the dynamics of paediatric immunization acceptance. *Scientific Reports, 5(1),* 10724.

28. Hota, A. R., Sundaram, S. (2019). Game-theoretic vaccination against networked sis epidemics and impacts of human decision-making. *IEEE Transactions on Control of Network Systems, 6(4),* 1461–1472.
29. Li, X. J., Li, X. (2020). Perception effect in evolutionary vaccination game under prospect-theoretic approach. *IEEE Transactions on Computational Social Systems, 7(2),* 329–338.
30. Poletti, P., Caprile, B., Ajelli, M., Pugliese, A., Merler, S. (2009). Spontaneous behavioural changes in response to epidemics. *Journal of Theoretical Biology, 260(1),* 31–40.
31. Attaullah, Ramzi, D., Weera, W. (2022). Galerkin time discretization scheme for the transmission dynamics of hiv infection with non-linear supply rate. *AIMS Mathematics, 6,* 11292–11310.
32. Attaullah, Alyobi, S., Yassen, M. F. (2022). A study on the transmission and dynamical behavior of an hiv/aids epidemic model with a cure rate. *AIMS Mathematics, 7(9),* 17507–17528.
33. Wang, L., Schuetz, C. G., Cai, D. (2021). Choosing response strategies in social media crisis communication: An evolutionary game theory perspective. *Information & Management, 58(6),* 103371.
34. Wang, J., Wang, X., Fu, L. (2020). Evolutionary game model of public opinion information propagation in online social networks. *IEEE Access, 8,* 127732–127747.
35. Molinero, X., Riquelme, F. (2021). Influence decision models: From cooperative game theory to social network analysis. *Computer Science Review, 39,* 100343.
36. Li, S., Qu, S. (2023). The three-level supply chain finance collaboration under blockchain: Income sharing with shapley value cooperative game. *Sustainability, 15(6),* 5367.
37. Jiang, C., Chen, Y., Liu, K. R. (2014). Graphical evolutionary game for information diffusion over social networks. *IEEE Journal of Selected Topics in Signal Processing, 8(4),* 524–536.
38. Li, Y., Zhao, H. V., Chen, Y. (2022). Graphical evolutionary game theoretic modeling of strategy evolution over heterogeneous networks. *IEEE Transactions on Signal and Information Processing over Networks, 8,* 739–754.
39. Simon, H. A. (1955). A behavioral model of rational choice. *The Quarterly Journal of Economics, 69(1),* 99–118.
40. Wakker, P. P. (2010). *Prospect theory: For risk and ambiguity*. Cambridge, UK: Cambridge University Press.
41. Kephart, J. O., White, S. R. (1992). Directed-graph epidemiological models of computer viruses. In: *Computation: The micro and the macro view*, pp. 71–102. Hackensack, NJ, USA: World Scientific.
42. Wu, J. T., Leung, K., Leung, G. M. (2020). Nowcasting and forecasting the potential domestic and international spread of the 2019-nCoV outbreak originating in Wuhan, China: A modelling study. *The Lancet, 395(10225),* 689–697.
43. Zhu, S., Srebric, J., Spengler, J. D., Demokritou, P. (2012). An advanced numerical model for the assessment of airborne transmission of influenza in bus microenvironments. *Building and Environment, 47,* 67–75.
44. Foster, A., Kinzel, M. (2021). Estimating COVID-19 exposure in a classroom setting: A comparison between mathematical and numerical models. *Physics of Fluids, 33(2),* 021904.
45. Traulsen, A., Claussen, J. C., Hauert, C. (2004). Coevolutionary dynamics: From finite to infinite populations. *Physical Review Letters, 95(23),* 238701.
46. Karlsson, C. J., Rowlett, J. (2020). Decisions and disease: A mechanism for the evolution of cooperation. *Scientific Reports, 10(1),* 13113.
47. Lyapunov, A. M. (1992). The general problem of the stability of motion. *International Journal of Control, 55(3),* 531–534.
48. Chakrabarti, D., Wang, Y., Wang, C., Leskovec, J., Faloutsos, C. (2008). Epidemic thresholds in real networks. *ACM Transaction on Information and System Security, 10(4),* 1–26.
49. Toczyski, P., Banerski, G. (2021). Patterns of digital users' irrationality in the moment of digital transformation of the media. In: *Digital interaction and machine intelligence*, pp. 115–124. Springer International Publishing.

50. Gogtay, N. J., Thatte, U. M. (2017). Principles of correlation analysis. *Journal of the Association of Physicians of India, 65(3),* 78–81.
51. Senthilnathan, S. (2019). Usefulness of correlation analysis. *SSRN Electronic Journal*. https://doi.org/10.2139/ssrn.3416918
52. Dryhurst, S., Schneider, C. R., Kerr, J., Freeman, A. L., Recchia, G. et al. (2022). Risk perceptions of covid-19 around the world. In: *COVID-19*, pp. 162–174. London, UK: Routledge.
53. Bruine de Bruin, W., Saw, H. W., Goldman, D. P. (2020). Political polarization in us residents' COVID-19 risk perceptions, policy preferences, and protective behaviors. *Journal of Risk and Uncertainty, 61,* 177–194.